University of Tartu

Faculty of Science and Technology

Institute of Ecology and Earth Sciences

Department of Geography

Master Thesis in Geoinformatics for Urbanized Society

Estimating hemi-boreal forest productivity with a process-based BEPS model and multi-source Earth Observation data

Author: Fariha Harun

Supervisors: Dr. Jan Pisek

Dr. Kaido Soosaar

Tartu 2021

Annotatsioon

Primaarproduktsioon on globaalse maapealse süsinikuringe ja kliimamuutuste põhikomponent. Antud uurimuses hinnati primaarproduktsiooni muutusi, kasutades boreaalse ökosüsteemi tootlikkuse simulaatori (BEPS) mudelit, et kontrollida Soontaga piirkonna näitel mudeli jõudlust Eesti hemiboreaalsetes metsades. Mudeli käitamiseks kasutati kombinatsiooni kaugseirest (lehepinnaindeks, *clumping* indeks) ja meteoroloogilistest andmetest (temperatuur, kiirgus, õhuniiskus, sademed ja tuulekiirus). Tulemuste kinnitamiseks kasutati Soontaga uurimisjaamas mõõdetud primaarproduktsiooni andmeid. Hinnati ka uurimisala ruumilist sobivust. Tulemused näitasid, et sobiva, usaldusväärse ja kvaliteetse andmestiku olemasolul jälgib BEPS-mudel edukalt primaarproduktsiooni sesoonseid muutusi ja aastatevahelisi variatsioone hemiboreaalses metsas.

Märksõnad: primaarproduktsioon, BEPS-mudel, lehepinnaindeks, ruumiline sobivus, hemiboreaalne mets

CERCS- P510 (Füüsiline geograafia, geomorfoloogia, mullateadus, kartograafia, klimatoloogia)

Abstract

Gross Primary Productivity (GPP) is the core component of terrestrial carbon cycle as well as the global carbon cycle and earth climate research. In this study, GPP estimation was performed by Boreal Ecosystem Productivity Simulator (BEPS) model to explore BEPS model’s performance for Estonian hemi-boreal forests on an example of the Soontaga area. The model was run by using the combination of remote sensing (leaf area index (LAI), clumping index) and meteorological data inputs (temperature, radiation, humidity, precipitation and windspeed). The results were validated against the tower measured GPP at Soontaga. The spatial representativeness of the site was evaluated as well. It was found that BEPS model track the GPP changes with season and inter-annual variation very well in a hemi-boreal region given that good, reliable quality input data are provided.

Keywords: GPP, BEPS, LAI, spatial representativeness, hemi-boreal forest.

CERCS- P510 (Physical geography, geomorphology, pedology, cartography, climatology)

Table of Contents

Abbreviation

Abbreviation	**Details**
APAR	Absorbed Photosynthetically Active Radiation
BEPS	Boreal Ecosystem Productivity Simulator
CO_2	Carbon Dioxide
EC	Eddy Covariance
EO	Earth Observation
GPP	Gross Primary Productivity
LAI	Leaf Area Index
LUE	Light Use Efficiency
NPP	Net Primary Productivity
RMSE	Root Mean Square Error

1. Introduction

The terrestrial carbon (C) cycle is one of the most important focus areas in research on global climate change (Feng et al., 2007). It includes the exchange of carbon among the terrestrial biosphere, pedosphere, geosphere, and atmosphere of the Earth. Plants absorb carbon from the atmosphere through photosynthesis and store it in biomass (leaves, branches, trunks, and roots). Photosynthesis is the way for the terrestrial ecosystem to sequester carbon dioxide (CO_2). During this process, it also releases the carbon back into the atmosphere through autotrophic respiration (Xiao et al., 2019).

In the terrestrial C cycle, the key component is gross primary production (GPP) along with respiration (Feng et al., 2007). GPP can be defined as the total amount of carbon uptake by vegetation through photosynthesis which is the largest global carbon flux (Li et al., 2016) and which drives several ecosystem functions such as respiration and growth (Beer et al., 2010). GPP is the basis for food, fiber, and wood production and by this way it is contributing to human welfare as well as representing a key component of the carbon cycle (Xiao et al., 2019). One of the major processes of controlling land-atmosphere CO_2 exchange is completed by GPP and it provides the capacity of terrestrial ecosystems to partly offset anthropogenic CO_2 emissions (Beer et al., 2010). GPP consists of Net Primary Productivity (NPP) and autotrophic respiration (Liu et al., 1999). NPP defines the difference between accumulated photosynthesis and accumulated autotrophic respiration through green plants per unit time and space (Feng et al., 2007). NPP refers to the total amount of carbons added to plant biomass per unit of space and time. Productivity is very vital to ecology as well as carbon storage by land ecosystems and it can play an important role in limiting the rate of atmospheric CO_2 increase (Feng et al., 2007).

Understanding the controlling mechanism of terrestrial GPP is very important as well as understanding its accurate estimation process (Li et al., 2016). Significant change arises in the atmospheric CO_2 concentration if any fluctuation occurs in terrestrial GPP, because GPP is directly connected to the carbon cycle and global climate change (Anav et al., 2013; Prentice et al., 2000). By continuous monitoring and accurate GPP estimation the long-term sustainability of terrestrial ecosystem services can be ensured. Accurate estimation helps to address topics which are affecting the global carbon cycle together with determining the size of the terrestrial carbon sink, vegetation dynamics prediction, and forests and grasslands management (Shi et al., 2017). Accurate estimation of GPP of terrestrial ecosystems for regions, continents as well as the globe can help to improve our understanding about the conditions of the terrestrial biosphere and facilitate the policymaker for better climate policymaking (Wu et al., 2010).

Despite its importance, there are persisting uncertainties and inconsistencies in GPP estimation between different models (Li et al., 2016). One possible reason for the inconsistency in the estimation of GPP is insufficient model parametrization or structural model errors which leads to GPP overestimation (Beer et al., 2010). On the other hand, underestimation of GPP may be caused by not including the positive effects of nitrogen disposition (Li et al., 2016). Despite being a widely used product, MODIS GPP product is generally underestimating GPP by about 34% across all biomes (Zhu et al., 2018). Another possible reason for uncertainty is quality or deficiency of input data that have a great impact on the accuracy of estimation results (Feng et al., 2007). GPP estimation may have significant errors because of coarse resolution of climate inputs (Shi et al., 2017). For example, according to Feng et al. (2007), it is evident that LAI accuracy has a significant impact on NPP estimation as well as GPP estimation.

Several approaches have been developed to estimate spatial and temporal variations in terrestrial GPP: (1) light use efficiency (LUE) models, (2) process-based ecosystem models, and (3) machine learning upscaling models (Li et al., 2016). Feng et al., (2007) suggested three types of models, which are generally used to estimate terrestrial NPP as well as GPP: (1) statistical models, (2) parametric models, and (3) process-based models.

Another GPP estimation technique is the eddy covariance (EC) technique, which can estimate net CO_2 exchange under the ecosystem scales and that can be used for GPP calculation (Wu et al., 2010). In eddy covariance process, it measures the energy fluxes, water, and carbon which are in between the atmosphere and surface with a very high temporal (hourly, half hourly) frequency. For this reason, eddy covariance can provide invaluable prospects while evaluating the process-based models (Zhang et al., 2012).

The light use efficiency (LUE) model can effectively explain the spatial and temporal GPP dynamics. This model provides a straight proportionate relation between biological production and the amount of photosynthetically active radiation, which is absorbed by the vegetation canopy (APAR) (Wu et al., 2010). But in LUE estimation, the problem arises with the plant's functional verity, and the estimation can be affected by temperature, soil water content, vapor pressure deficit (VPD), and leaf phenology parameterization (Xiao et al., 2005). Besides, if the climate inputs of LUE models are in coarse resolution, it may cause error in GPP estimation and create hindrance in the way of acquiring the large-scale fine-resolution GPP estimates (Shi et al., 2017). Statistical models and parametric models are two simple and easily usable models. However, these two models can have strong limitations as they might not have proper theory and full, detailed understanding about the function of the given ecosystem (Feng et al., 2007).

Process models generally integrate the mechanisms to simulate numerous plant functional processes including photosynthesis, autotrophic respiration and transpiration, and various plant physiological processes together with photosynthesis, autotrophic respiration and transpiration (Feng et al., 2007). Process-based ecosystem models are also directly linked to other Earth system model's components as well as they can simulate historical and future global climate change projection in a systematic way (Li et al., 2016). On the other hand, in a process-based model, computing resources are challenging the modelers to trade-off between model execution time steps and spatial resolution. Despite some limitations, process-based models were found to provide more reliable results than other types of models (Feng et al., 2007).

Boreal Ecosystem Productivity Simulator (BEPS) model is a carbon-water coupled process model developed for Canadian boreal forest conditions, which is based on remote sensing inputs. The BEPS model consists of an advanced canopy radiation sub-model for quantifying the effects of canopy architecture on the radiation distribution and photosynthesis in the canopy (Feng et al., 2007). BEPS computes the total photosynthetically active radiation, which was absorbed by the canopy in each pixel. Also, with this model, it is possible to analyze light use efficiencies for GPP. BEPS integrates the input data and produces an output of GPP in the form of NPP and other carbon and water cycle components such as autotrophic respiration and evapotranspiration (Liu et al., 1999).

Observing and considering the spatial representativeness of the study area helps to get better understanding about the annual GPP and carbon stock (Ma et al., 2019). There may be a mismatch between spatial footprint area of the tower-based and satellite observations which generates a lot of challenge for directly comparing the point with pixel (Román et al., 2009). The gamma variance model has been identified an effective tool to explore the spatial variability of land surface and to assess the spatial representativeness and suitability of individual sites for comparison with satellite observations (Román et al., 2009). Using this approach, spatial characteristics of the study site can be then compared against the greater surrounding area and extend to a satellite pixel resolution. (Román et al., 2009)

1.1 Objective of the Study

The BEPS model has been originally developed and found very useful for estimating GPP of boreal forests. There are no existing, published studies with BEPS model tested over Estonia or in hemi-boreal region in general. The objective of this study is to evaluate potential suitability of BEPS model and input remote sensing data for GPP estimation over hemi-boreal forests using the available GPP measurements from the Soontaga flux tower site. The following steps are taken to achieve this objective: first, the spatial heterogeneity of the Soontaga site is assessed with 30 m resolution remote sensing data. Next, the BEPS model is evaluated by comparing GPP estimates with the tower measurements under different weather conditions (dry/wet) over several years (2016-2019). The study period covering several years, and different weather conditions shall provide sufficiently different scenarios to assess the full performance of BEPS model and its overall suitability for hemi-boreal region.

1.2 Research Questions

The research questions for this study are:

a. How spatially heterogenous is the Soontaga flux tower area?
b. How much reliable GPP information can be simulated by the BEPS compared to estimates obtained with the tower eddy covariance measurements taken at the Soontaga site?
c. How well can the BEPS model track the GPP changes with season and inter-annual variation?

2. Materials and Methods

2.1 Study area description

The Soontaga flux tower (58°01'24 "N, 26°04'15"E) is located in a dry hemi-boreal forest dominated by Scots pine (*Pinus sylvestris*) (Krasnova et al., 2019). Soontaga area is a coniferous forest site of Vaccinium type where the stand age was approximately 60-210 years with the maximum canopy height of 30 m and the existing second layer of *Picea abies* with average height of 15 m. Mean annual temperature was 7.2℃, with mean annual sum of precipitation about 728 mm in 2019 (Estonian Environment Agency (KAUR)). The location of the study area and tower is shown in Figure 1.

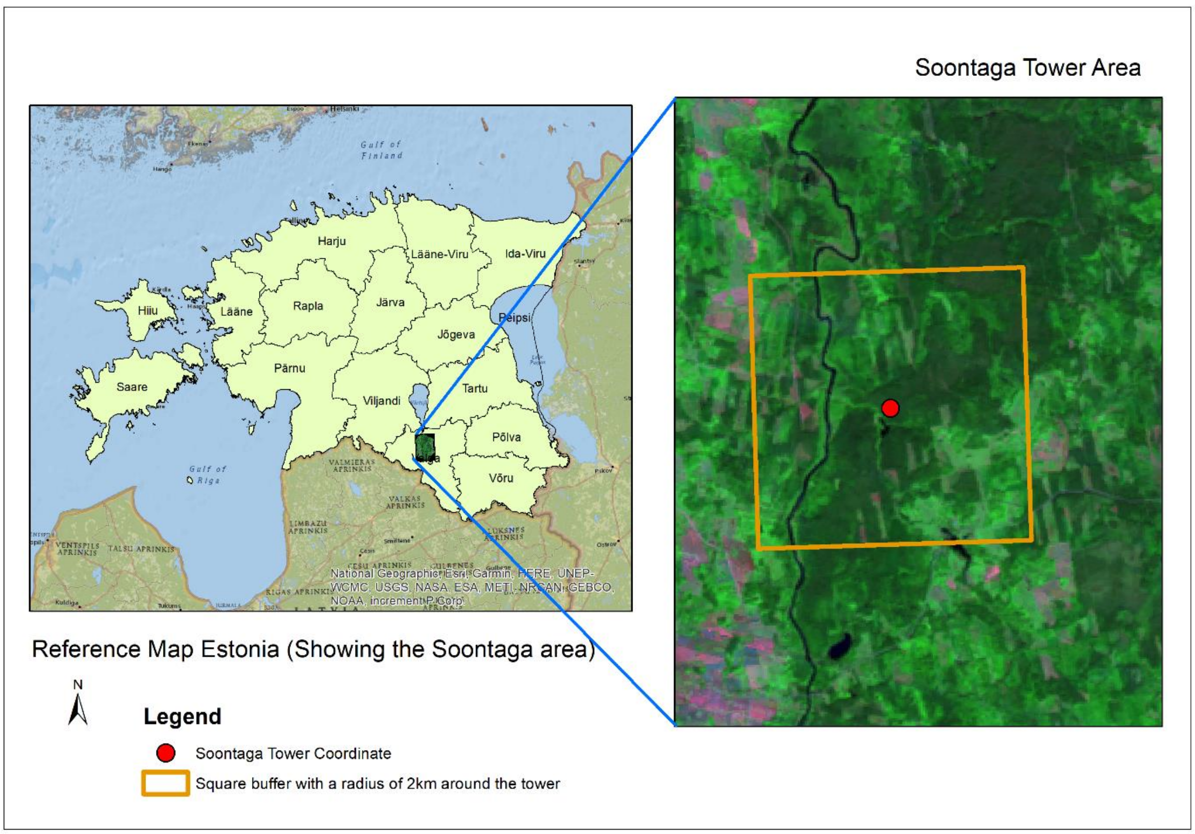

Figure 1. Study area map with 2 km rectangle buffer around the tower (The background image in panel 2 is the Landsat image used for the spatial representativeness analysis in section 3.1).

2.2 Spatial representativeness of flux tower area

Gamma variance model has been identified as an effective tool for assessing the spatial representativeness (Román et al., 2009). Following Román et al. (2009) and Wang et al. (2012, 2014), the surface heterogeneity was evaluated using the surface albedo retrievals from a 30 m spatial resolution Landsat data as an input to the model. The surface albedo has been obtained by the narrowband-to-broadband conversion (Liang et al., 2003; Smith, 2010):

$$A = \frac{0.356p_1 + 0.130p_3 + 0.373p_4 + 0.085p_5 + 0.072p_7 - 0.0018}{0.356 + 0.130 + 0.373 + 0.085 + 0.072} \quad \text{(eq. 1)}$$

where p_i are respective Landsat 7 bands. The spatial representativeness at different scales was assessed by calculating the gamma variance with 500 m, 1 km, 1.5 km, and 2 km footprint areas centered at the flux tower (Figure 2).

The gamma variance estimator, $y_E(h)$ was used to attain half the average square difference between albedo values, which are within a specific distance, classes, or bins and these are defined by the multiplication of 30 m (Román et al., 2009):

$$y_E(h) = 0.5\frac{\sum(Z_{xi} - Z_{xi})^2}{N(h)} \quad \text{(eq. 2)}$$

Here, Z_{xi} refers the surface albedo at the pixel location of x; and Z_{xi+h} corresponds to the surface albedo at another pixel which should be within a lag distance h. The maximum lag distance which is used in each gamma variance is constrained by the half maximum distance of the given subset and have to be a factor of the minimum lag (i.e., 30 m) as a thumb rule (Román et al., 2009). Thus, for a 1.0 km^2 subset h_{max} = 690 m, for a 1.5 km^2 subset h_{max} = 1050 m, 2 km^2subset h_{max} = 1410 m.

2.3 BEPS model description

The BEPS model consists of an advanced canopy radiation sub-model for quantifying the effects of canopy architecture on the radiation distribution and photosynthesis in the canopy (Feng et al., 2007). BEPS computes the total photosynthetically active radiation, which was absorbed by the canopy (Liu et al., 1999). The sunlit and shaded leaf separation approach strategy (Chen et al.,

1999) has been used in the BEPS model (Liu et al., 2002). The stratification strategy is preferred in the BEPS model over other strategies (Bonan, 1995) because it captures the key radiation variation inside the canopy allows effective temporal integration (Chen et al., 1999) during a given time.

The total GPP can be calculated with the separation of sunlit and shaded leaf groups based on the daily canopy (Liu et al., 2002):

$$GPP = (A_{sun}\, LAI_{sun} + A_{shade}\, LAI_{shade}) \quad \text{(eq. 3)}$$

In Eq. (3), the subscripts' sun' and 'shade' denote sunlit and shaded components, A is the daily mean of photosynthesis rate, and LAI is leaf area index. The GPP output unit of BEPS model is g Cm^{-2} per day.

Mean photosynthesis rate A can be obtained with Eq. (4) where the calculation is carried separately for sunlit and shaded leaves (Liu et al., 1999):

$$A = \frac{1.27}{2(g_n - g_{min})}\left(\frac{a^{1/2}}{2}(g_n{}^2 - g_{min}{}^2) + c^{1/2}(g_n - g_{min}) - \frac{2ag_n + b}{4a}d + \frac{2ag_{min} + b}{4a}e + \left(\frac{b^2 - 4ac}{8a^{3/2}}\right)\ln\frac{2ag_n + b + 2da^{1/2}}{2ag_{min} + b + 2ea^{1/2}}\right) \quad \text{(eq. 4)}$$

Here, A is the minimum of Rubisco-limited photosynthesis rate A_C and light limited photosynthesis rate A_J in $\mu mol\ m^{-2}\ s^{-1}$.

For A_c:

$a = (k + C_{\mathrm{a}})^2$,

$b = 2(2\Gamma + K - C_{\mathrm{a}})V_m + 2(C_{\mathrm{a}} + K)R_d$,

$c = (V_m - R_d)$

For A_j:

$a = (2.3\Gamma + C_{\mathrm{a}})^2$,

$b = 0.4(4.3\Gamma - C_{\mathrm{a}})J + 2(C_{\mathrm{a}} + 2.3\Gamma)R_d$,

$c = (0.2J - R_d)^2$.

For both:

$d = (ag_n{}^2 + bg_n + c)^{1/2}$,

$e = \left(ag^2{}_{min} + bg_{min} + c\right)^{1/2}$ (Liu et al., 2002).

In the calculation, the R_d refers to the daytime leaf dark respiration in $\mu mol\ m^{-2}\ s^{-1}$(Liu et al., 2002). Besides, the enzyme kinetics function is in Pa which is represented by *K, Γ* is in in Pa unit and it represents the CO_2 compensation point when the dark respiration is absent (Zhang et al., 2012). Here, J is the electron transport rate, and its unit is $\mu mol\ m^{-2}\ s^{-1}$. The V_m denotes the maximum carboxylation rate in $\mu mol\ m^{-2}\ s^{-1}$ unit (Liu et al., 2002). According to Liu et al. (1999), inside the calculation procedure, both parameters, *Γ* and *K* are temperature-dependent, the stomatal conductance is assumed zero and minimum is denoted as g_{min}. The stomatal conductance is in $\mu mol\ m^{-2}\ s^{-1}$ unit and it is dependent upon radiation, air temperature, air humidity and soil water condition during the day (Liu et al., 1999).

Being a two-leaf model (Chen et al., 2012), the BEPS needs to calculate GPP separately for sunlit (LAI_{sun}) and shaded (LAI_{shade}) leaves:

$$LAI_{sun} = 2\cos\theta(1 - \exp(-0.5\Omega LAI/cos\theta) \quad \text{(eq. 5)}$$

$$LAI_{shade} = LAI - LAI_{sun} \quad \text{(eq. 6)}$$

Here,

$$\theta = \frac{1}{2}\left[\frac{1}{2}\left(\frac{\pi}{2} + \theta_{noon}\right)\right] = \frac{\pi}{8} + \frac{3}{4}\theta_{noon} \quad \text{(eq. 7)}$$

$$\theta_{noon} = \frac{\pi}{180}\left[lat - 23.5 * \sin(julianday - 81) * 2 * \frac{\pi}{365}\right] \quad \text{(eq. 8)}$$

Here, θ represents solar zenith angle, θ_{noon} stands for solar zenith angle at noon and lat represents latitude, Ω represents clumping index. Clumping index describes the aggregation of the foliage elements within a canopy. The random distribution would equal 1; clumping index with values less than one indicates more clumped vegetation (Nilson, 1971).

2.4 Input data for the BEPS

The input data required for BEPS are leaf area index (LAI), land cover, clumping index, and daily meteorological data (Feng et al., 2007).

The LAI input data was acquired from MODIS 4-day MCD15A3H.006 collection with 500m resolution for four years period (from 2016 to 2019). This data was generated using the algorithm which chooses the "best" pixel offered by both MODIS sensors located on NASA's Terra and Aqua satellites and the data was scaled with factor for 0.1. After downloading the MODIS LAI, the original LAI values were interpolated linearly to daily steps. The LAI values used for the model cover the time range from January 2016 to December 2019. The MODIS LAI values were observed to occasionally reach up to maximum value of 6 which is not realistic for the tower area. But LAI value of 3 was previously found to be a maximum value at a comparable Scots pine stand in Järvselja, Estonia (Pisek et al., 2011). The input LAI values were capped at value of 3 to provide a more realistic scenario to be encountered at the Soontaga site. Evergreen needleleaf land cover type class and the value of 0.69 as the clumping index provided for the location in the global map by He et al. (2012) were used in this study.

The necessary meteorological data for the BEPS model include temperature, humidity, radiation, precipitation, and wind speed information (Liu et al., 1997). In this study all the input meteorological data are required with an hourly step. All the meteorological data used in this study were collected directly from the tower site and provided by the Department of Natural and Exact Sciences, Institute of Ecology and Earth Sciences, University of Tartu. The missing meteorological values were interpolated and converted to the hourly values from half hourly values.

2.5 Tower GPP calculations

Tower GPP values were obtained from eddy-covariance $CO2$ fluxes using nighttime-data-based flux partitioning method in REddyProcWeb online tool (Wutzler et al., 2018; Reichstein et al., 2005). Nighttime (Rg < 10 Wm^{-2}) net ecosystem exchange (NEE) values are fully represented by nighttime ecosystem respiration (ER) and GPP is set to zero. Here, calculated daytime GPP is obtained as a difference between measured daytime NEE and modeled daytime ecosystem respiration (ER). Lloyd & Taylor (1994) regression model were fitted to the nighttime ER data using air temperature as the driving factor. Model parameters estimated from the nighttime data with a sliding 7-days window and daytime air temperature were then used to model daytime ER (Lloyd & Taylor, 1994).

3. Results and Discussion

3.1 Spatially heterogeneity analysis of the flux tower area

Figure 3 presented the geostatistical assessment of the site heterogeneity assessed at three different scales (0.5 km, 1 km, 1.5 km, 2 km). The gamma variance for the 0.5 km footprint area (the nominal spatial resolution of the satellite input data) around the tower plateaus at 0.0003. According to Wang et al. (2017), if the gamma variance levels off at value less than 0.0005, the site can be deemed spatially representative. The Soontaga area within the 500 m distance from the tower can be considered spatially homogeneous and the tower footprint (20.88 ha) as well as the nominal resolution of the used remote sensing data. On the other hand, the gamma variance values for the distances of 1 km, 1.5 km and 2 km level off at values > 0.0005 (Figure 3). Based on the gamma variance values, the Soontaga site might not be representative of greater area (≥ 1km) as the gamma variance is over the suggested homogeneity threshold by Wang et al. (2017). It shall be also noted that the MODIS 500 m resolution products are actually generated from multi-angular observations that may come from a larger area (Wang et al., 2017) and could be thus influenced by the heterogeneity at and the greater area around the Soontaga tower.

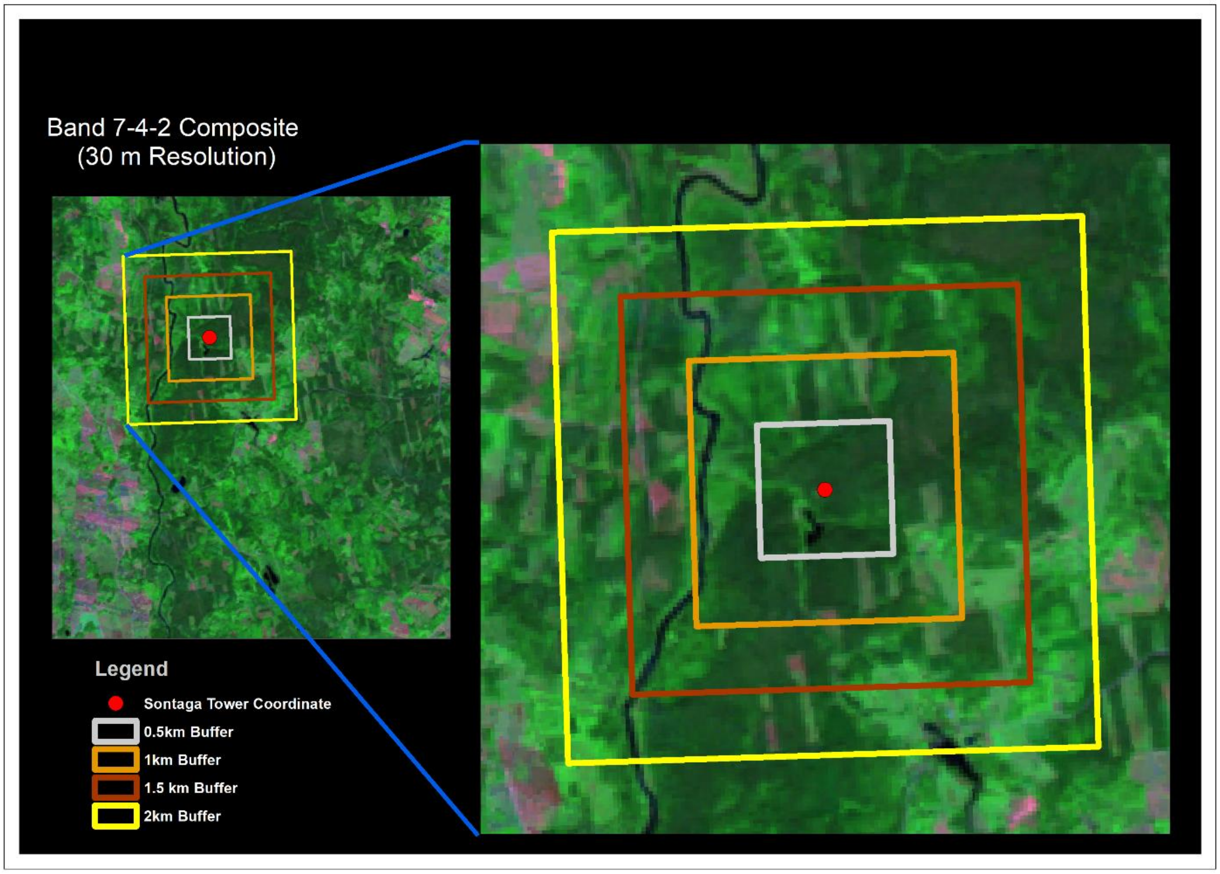

Figure 2. Spatial representativeness assessment map of Soontaga area.

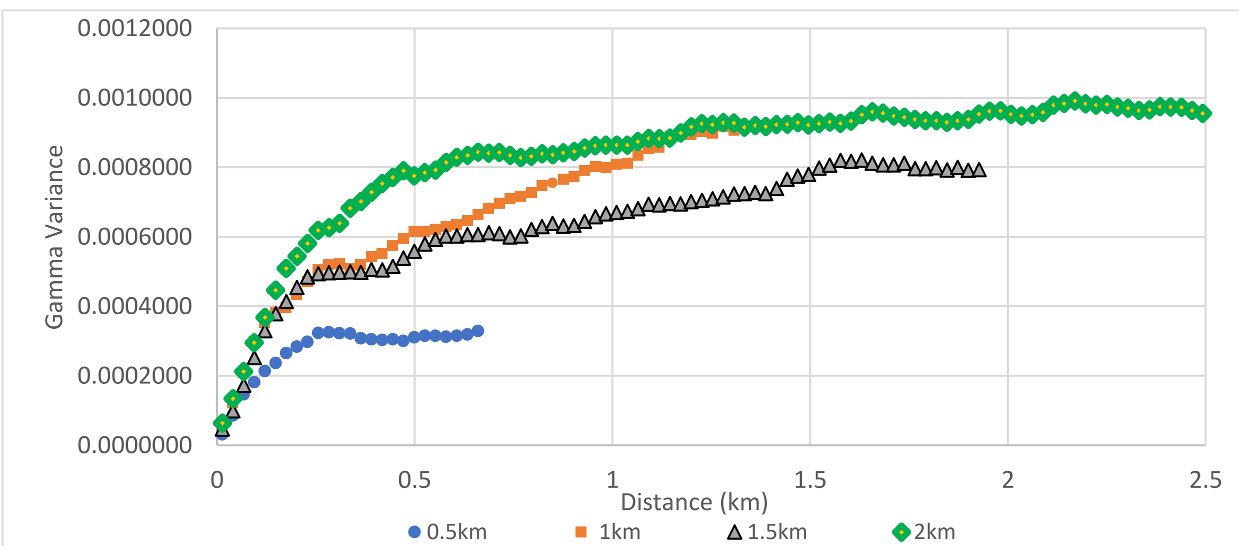

Figure 3. Gamma variance of surface albedo derived from Landsat 7 image taken on 1.07.2018.

3.2 BEPS model validation and comparison

The flux tower measurements were used to validate the BEPS result for each year. Table 1 provides the general performance overview of the GPP values obtained with the BEPS model and with the eddy covariance data measured at the site. Very close match is observed in 2017 and 2019. There was an excellent agreement (only 0.33% difference) in total GPP obtained with BEPS (1293.28 $\mathrm{g\,Cm^{-2}}$) and tower measurements (1288.96 $\mathrm{g\,Cm^{-2}}$) in 2019 with the root mean square error (RMSE) of 1.47. Similarly, only a 3.96% difference was observed in 2017, with GPP estimated by BEPS at 1214.34 $\mathrm{g\,Cm^{-2}}$and, tower GPP 1166.23 $\mathrm{g\,Cm^{-2}}$and RMSE of 1.51. Compared to the tower measurements, the BEPS model overestimated GPP by 16.98% in 2018 with RMSE of 2.42 and underestimated it by 23.12% with RMSE of 2.20 in 2016.

Table 1. Annual total GPP from tower-based observations, BEPS model; RMSE and percentage difference.

Year	GPP Tower ($\mathrm{g\,C\,m^{-2}}$)	GPP BEPS ($\mathrm{g\,C\,m^{-2}}$)	RMSE	Difference (%)
2019	1288.96	1293.28	1.47	0.33
2018	1143.96	1377.97	2.42	16.98
2017	1166.23	1214.34	1.51	3.96
2016	1447.61	1175.71	2.18	-23.12

More detailed comparison between tower values and BEPS and analysis of the factors affecting the performance and model agreement for each year is provided below.

3.3 Comparison of GPP values obtained with BEPS and EC tower measurements

The possible uncertainties in the tower based GPP estimations are discussed first, followed with the possible uncertainties in BEPS GPP calculation.

As discussed in Section 2.2, there may be a possible footprint mismatch between the tower eddy covariance measurements and scale resolution of BEPS input data. The eddy covariance tower data, that are used for the tower GPP estimates, generally represent fluxes with a footprint of typically 1 km × 1 km (Zhang et al., 2012). The footprint of Soontaga flux tower is 20.88 ha (Krasnova, prs. comm.), while the remote sensing data that are used to drive the BEPS model (LAI, clumping index) are provided at nominal 500 m resolution. The tower GPP estimates also have an uncertainty introduced during calculation steps (Liu et al., 2016). Mathematical methods are employed within the eddy covariance technique used to convert the measured CO_2 flux to GPP (Zhang et al., 2012). A manual mathematical conversion can sometimes cause uncertainties and fluctuation in the tower GPP values (Reichstein et al., 2005).

The meteorological or weather condition of the specific year can have impact on the BEPS model's performance. The bellow table provides an overview about the warm/cold and dry/wet condition of the years used in this study.

Table 2. Yearly seasonal conditions.

Year	Total yearly temperature sum (℃)	Total yearly precipitation (cm)	Warm/cold	Dry/wet
2019	72633.9	59.07	Warm	Wet
2018	71684.24	32.90	Warm	Dry
2017	62117.7	49.52	Cold	Wet
2016	66358.75	47.40	Cold	Wet

Based on meteorological data in Table 2, 2019 was the relatively warm and wet year compared to the other years included in this analysis. The site had enough water to support the process but at the same time high temperature causes high evaporation rate. The two opposite effects had kind of neutral effect and the GPP production was normal. There was a good match between BEPS and tower estimates throughout most of the seasonal course in 2019 (Figure 4). Compared to GPP values obtained with tower eddy covariance measurements, BEPS underestimated GPP from January to April and November to December. The Figure 8 shows that the LAI input values for BEPS are mostly zero during the first few months (till middle of April) as well as the last two months of the year. Since this is an evergreen needleleaf site, the actual LAI values were higher and allowed the photosynthesis process to start under suitable conditions which was captured by the eddy covariance measurements. In contrast, close to zero input LAI values provided to BEPS did not allow to match observed tower GPP values during these periods.

The GPP BEPS values were higher than the tower estimates from the middle of May to the middle of June 2019 (Figure 4). Compared to the beginning and towards the end of the year discussed above, input LAI values for BEPS did not suffer from underestimation during this period. The sharp increase in BEPS GPP values around 10 May coincides with the moment when the maximum LAI value, as provided by the MODIS LAI product, is reached. The period from the middle of May till the end of June may point to opposite effect compared to the start of the season. While the MODIS LAI product underestimated LAI over the site at the beginning of the season and consequently underestimated the GPP, the overestimated GPP by BEPS from the middle of the May till the beginning of July was caused by the apparent LAI overestimation in the MODIS LAI product during this section of the growing season. The maximum LAI for Scots pine stands was observed to be reached later in the season at the beginning of July (Heiskanen et al., 2012), compared to the earlier dates observed by the MODIS LAI product (Figure 8). This is also supported by an excellent agreement between the BEPS and tower based GPP estimates later in the season despite the similarly high MODIS LAI values are observed well till the end of August, which also agrees with the observations for Scots pine stands by Heiskanen et al. (2012).

Figure 5 is used to crosscheck the LAI impact. The model was tested with constant LAI values of 2 and 1 (Figure 5) as an input throughout the whole year. These two figures demonstrate a closer agreement between GPP BEPS and GPP estimates using tower observations from the beginning of the season till the beginning of July, confirming the LAI overestimation during the period by the MODIS LAI product was the cause of the disagreement between the BEPS and tower based GPP estimates.

The sudden, concurrent drops in GPP values predicted by both BEPS and tower observations are caused by the cloudy conditions, which limited the incoming irradiation below optimal levels for GPP production (Figure 9).

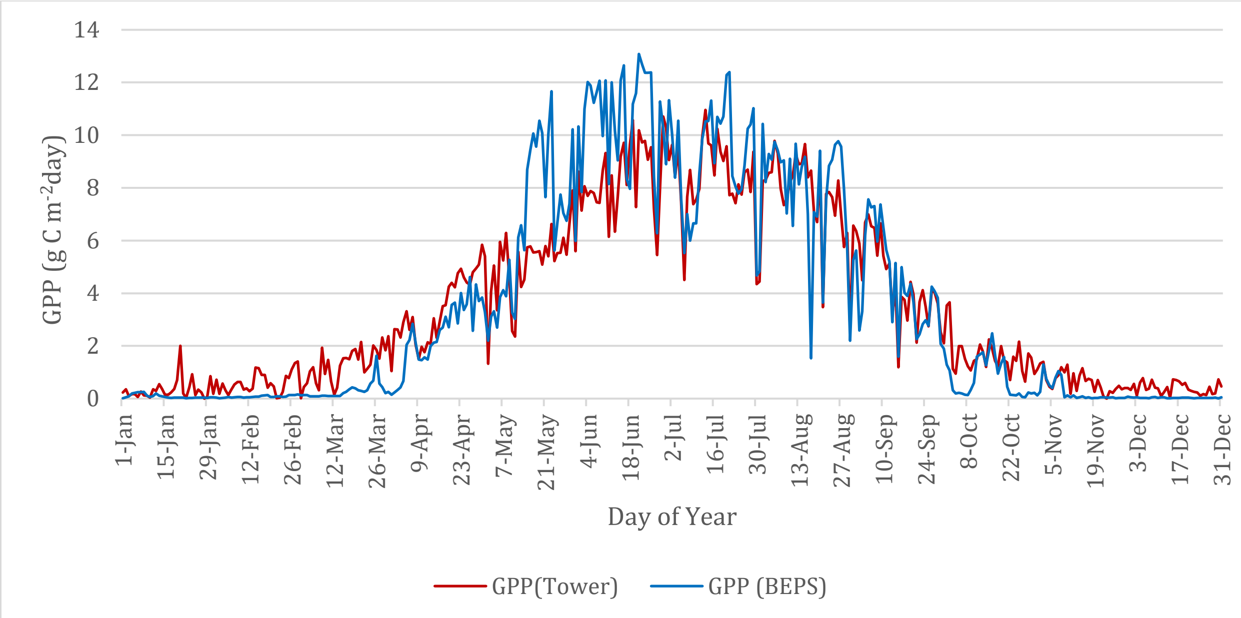

Figure 4. BEPS model and eddy covariance tower measurements in 2019.

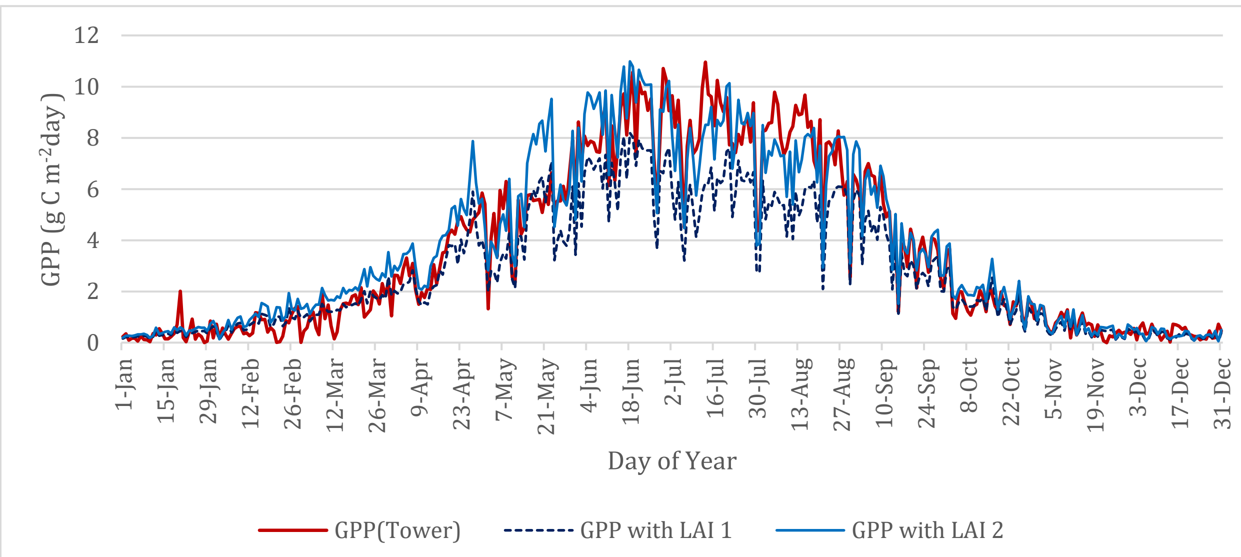

Figure 5. Eddy covariance tower measurements of GPP and predicted by BEPS in 2019 with setting LAI input as a constant at value of 1 and 2.

Daily BEPS GPP values are plotted against the tower GPP values in Figure 6. The Figure 6 shows a strong linear relationship reasonably close to 1:1 line with R square value of 0.89.

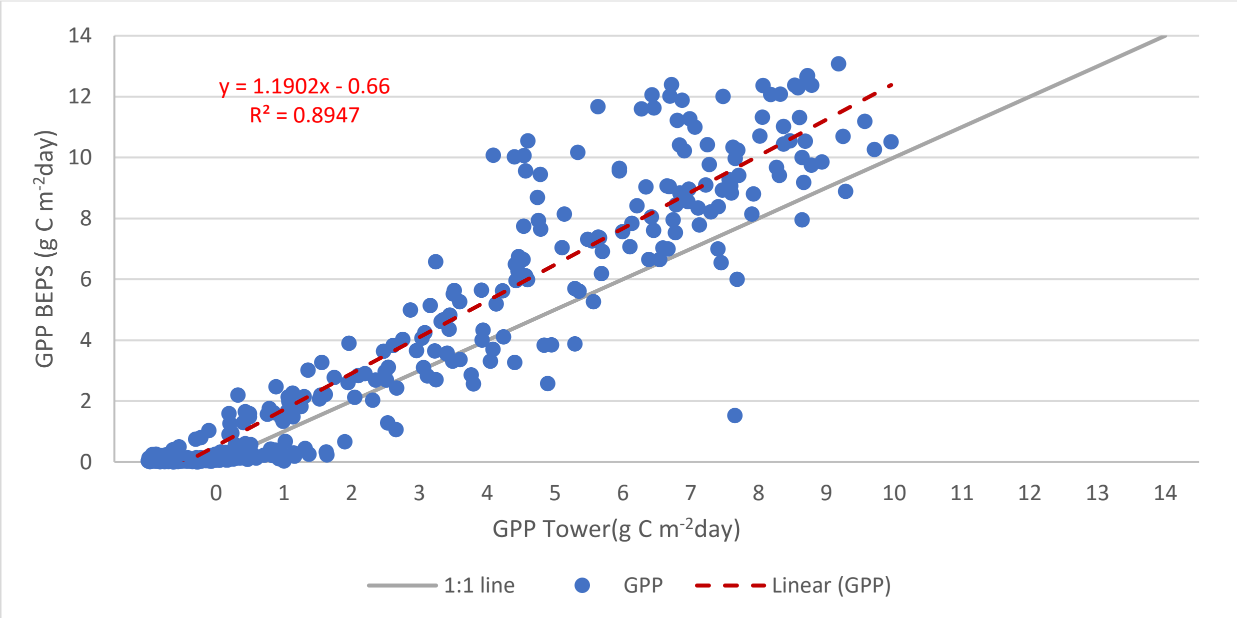

Figure 6. Comparison between BEPS and tower daily GPP estimates in 2019 (The solid line is 1:1 line and dashed one is a liner fit regression line).

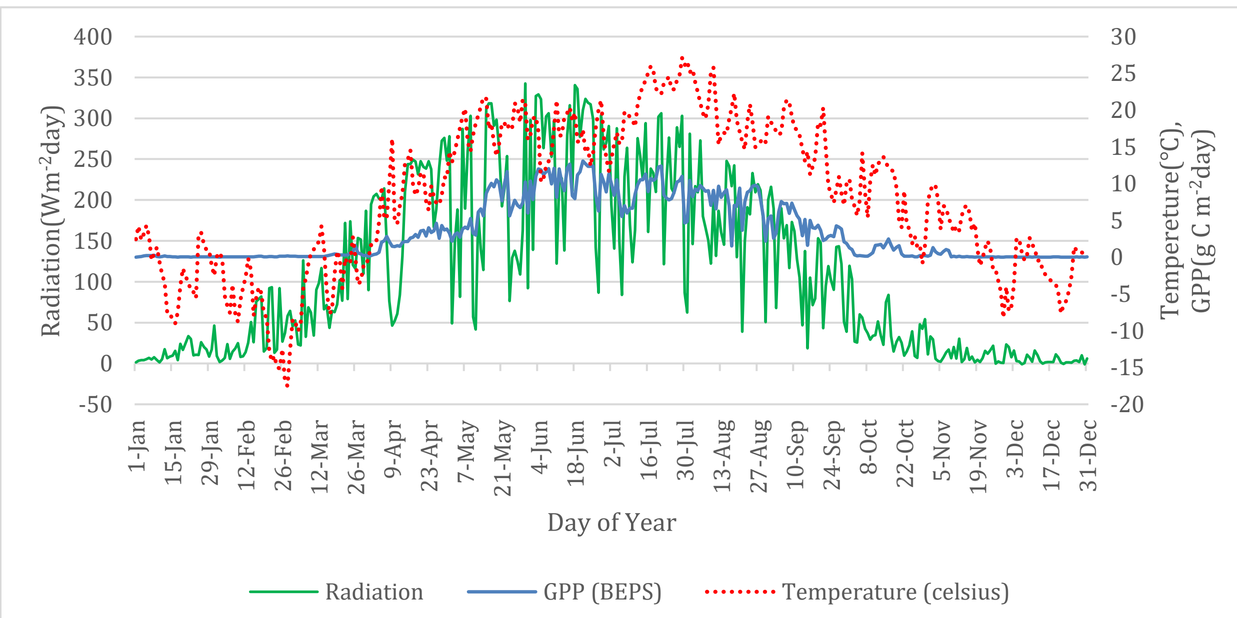

Figure 7. Radiation and temperature impact on BEPS GPP in 2019.

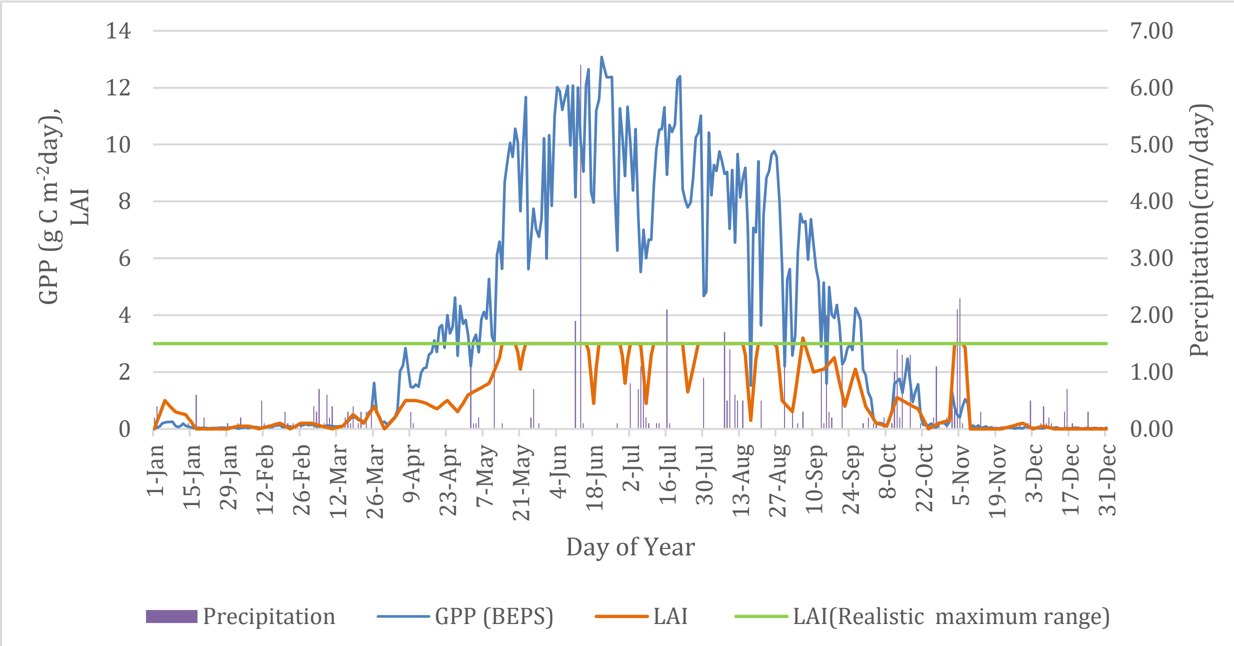

Figure 8. Seasonality impact on BEPS GPP in 2019.

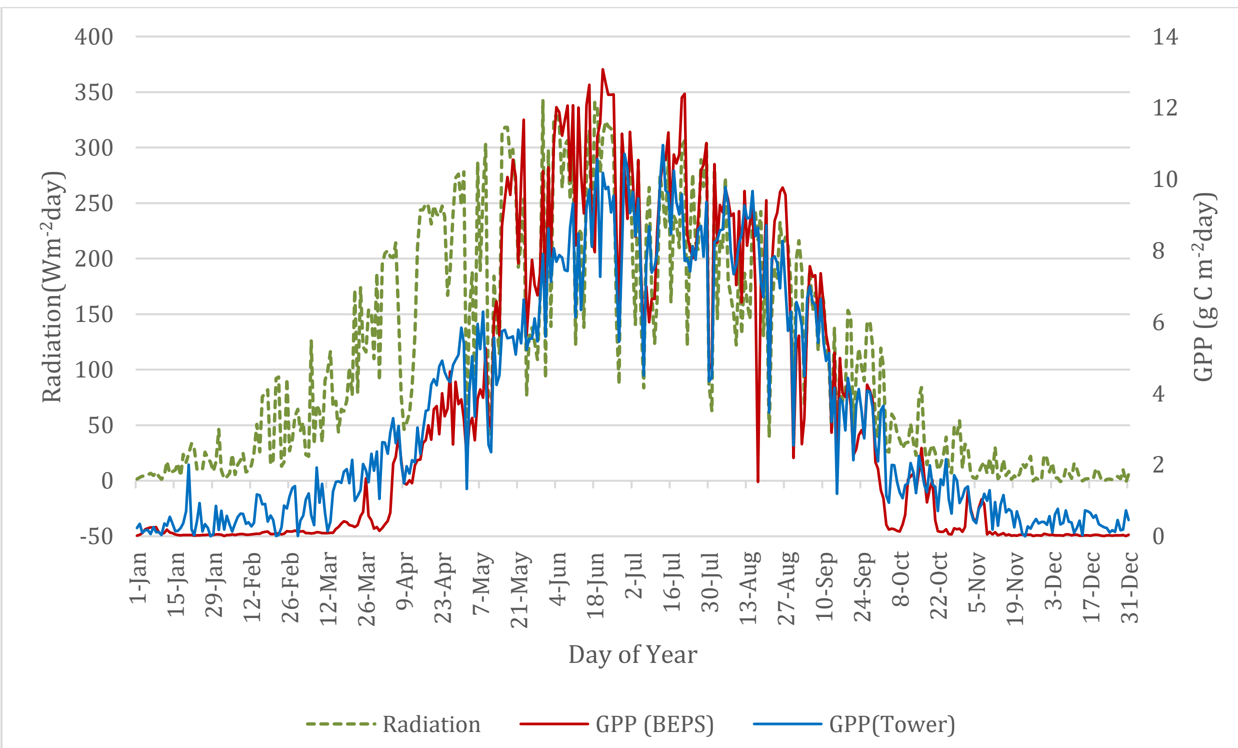

Figure 9. Effect of lower irradiation periods on the daily GPP fluctuation in 2019.

The year 2018 experienced drought during July at the Soontaga area (Estonian Weather Service), and the year was facing higher temperature than usual as well (Table 2). This caused relatively lower GPP production according to the tower-based measurements as there is less water to support the process because of dry weather and high temperature caused high evaporation. The BEPS GPP was matching the tower GPP very well at the very beginning and at the end of the growing season in 2018. BEPS model provided much higher GPP estimates compared to the tower GPP estimates for majority of the growing season period. The BEPS GPP course matches the radiation and temperature profiles very well (Figure 12) and when there is higher temperature it results in lower GPP predicted values. Figure 13 indicates low precipitation or dryness is behind the low BEPS GPP values. But similarly to 2019, the over-estimated LAI from the MODIS LAI product caused the over-estimation in the result of BEPS GPP from May to the third week of August. The first peak of BEPS over-estimation started from 7 May which matched the sudden increase in MODIS LAI values beyond the threshold LAI value of 3 which lasted with few exceptions till 17 August. The pronounced, sudden drops in both BEPS and tower based GPP estimates matched with big drop in LAI values in the MODIS product on 18 June (LAI value 0.9) and 24 July (LAI value 1.3) (Figure 13). Results from the 2018 season confirm clear, very high sensitivity BEPS to LAI input. GPP estimations by BEPS and tower-based observations show very good agreement during the main season where the MODIS product contains more realistic values that would better agree with the expected situation at the site (e.g., 24 July; LAI = 1.3).

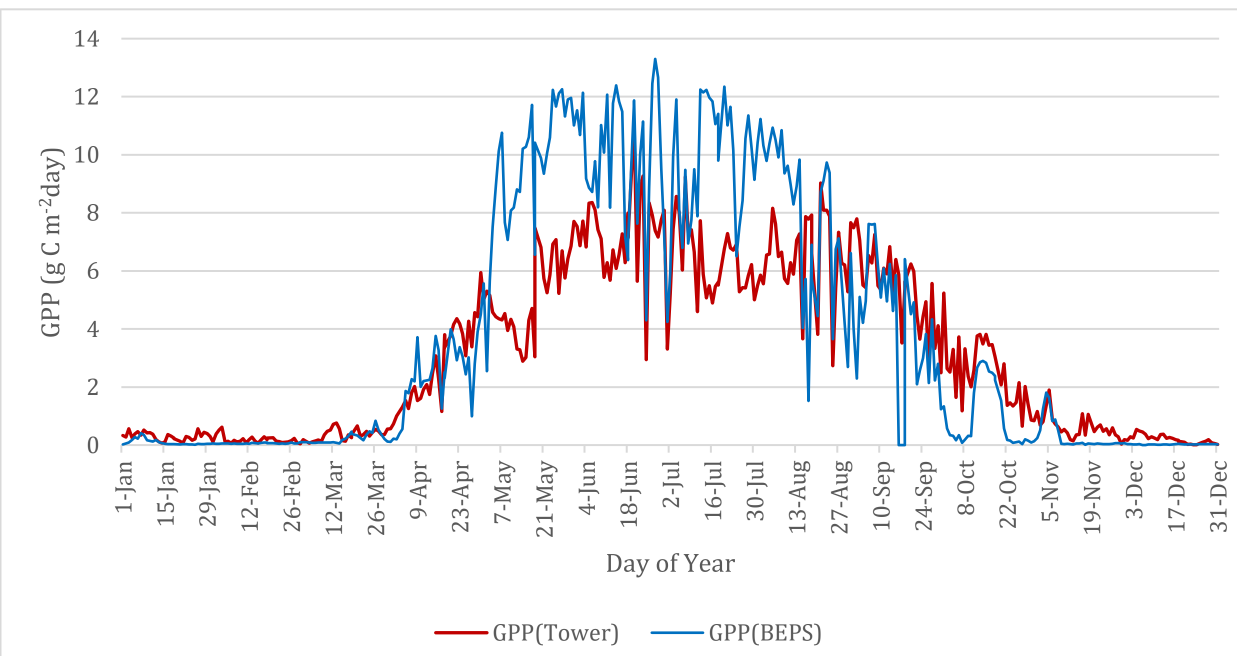

Figure 10. BEPS model and eddy covariance tower measurements in 2018.

Daily BEPS GPP values are plotted against the tower GPP values in Figure 11 with R square value of 0.754.

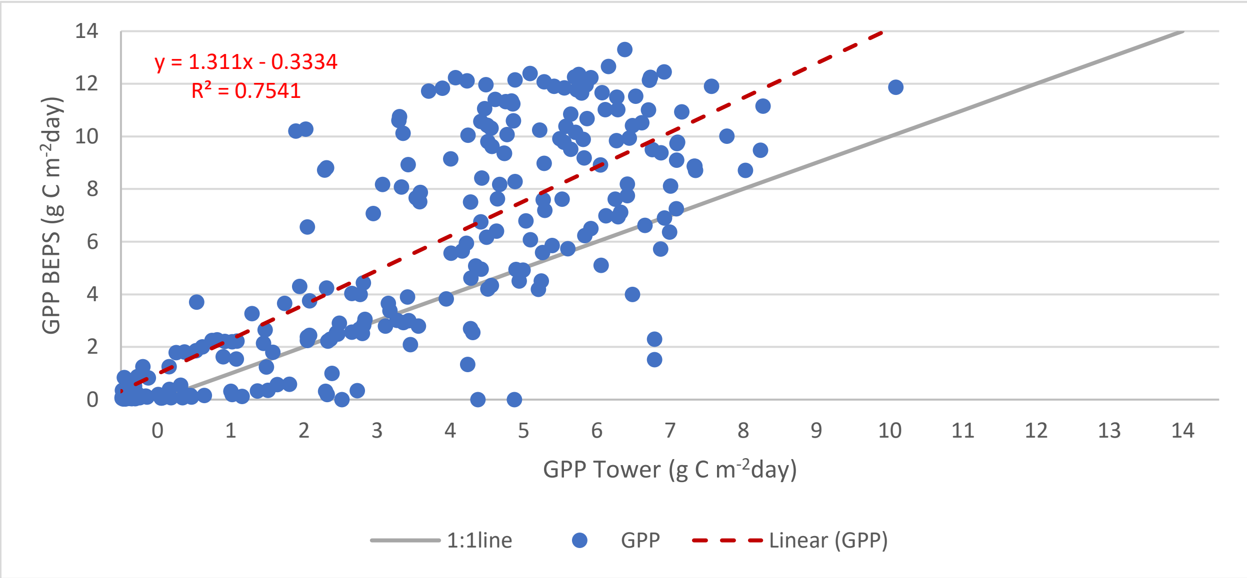

Figure 11. Comparison between BEPS and tower daily GPP estimates in 2018 (The solid line is 1:1 line and dashed one is linear fit regression line).

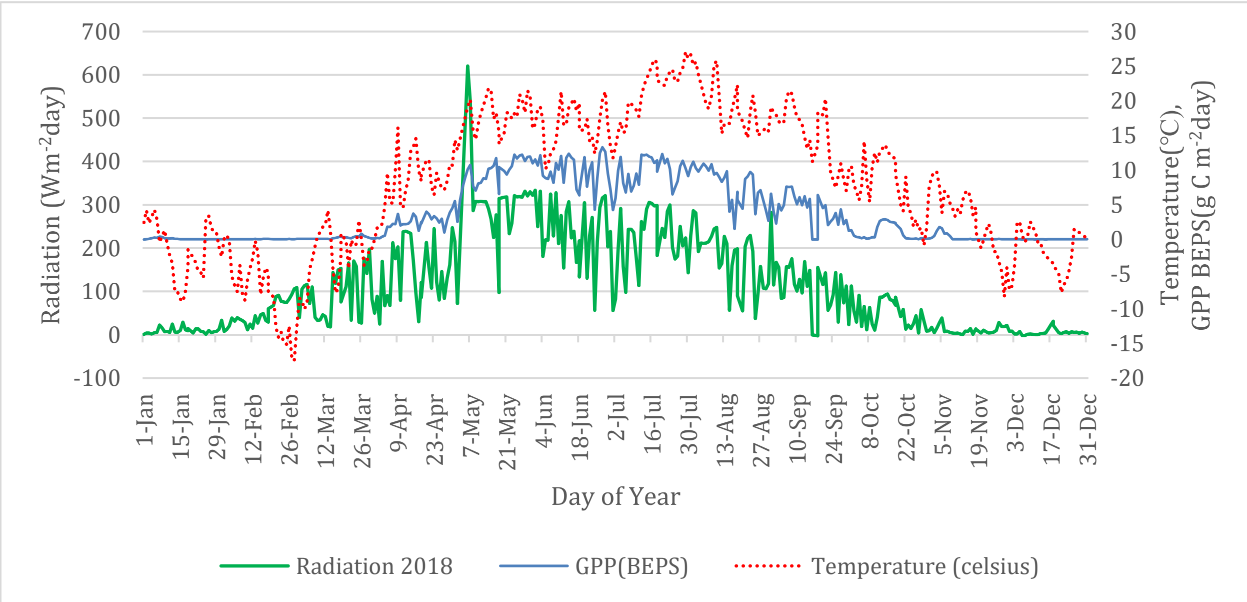

Figure 12. Radiation and temperature impact on BEPS GPP in 2018.

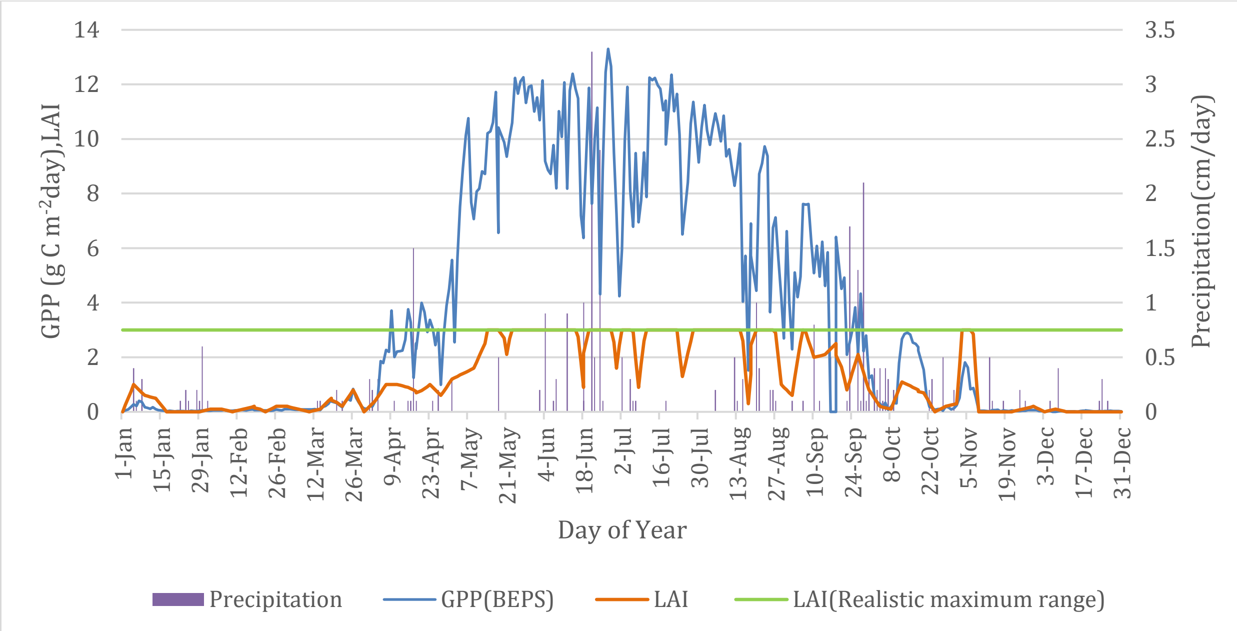

Figure 13. Seasonality impact on BEPS GPP in 2018.

Based on the meteorological data, the year 2017 was a relatively cold and wet year (Table 2) with much higher precipitation rate in autumn (Estonian Weather Service). There was again a very good match between the BEPS and tower based GPP values in 2017. Compared to tower-based estimates, the BEPS model over-estimated the yearly GPP sum by 3.96%. There was a close relationship with a very little difference between BEPS and tower estimates throughout the whole year (Figure 14). There are occasional small differences during the period from the last week of May to the third week of August (Figure 14). The GPP predictions by BEPS closely follow the seasonal temperature profile (Figure 16). Also, higher precipitation has a clear effect on higher GPP values (Figure 17). Similarly, to the situations in 2018 and 2019, the occasional small differences in BEPS GPP from last week of May to third week of August were caused by the apparent LAI overestimation by the MODIS LAI product during this part of the growing season. The differences in GPP (Figure 14) match with the timing of LAI saturation (Figure 17).

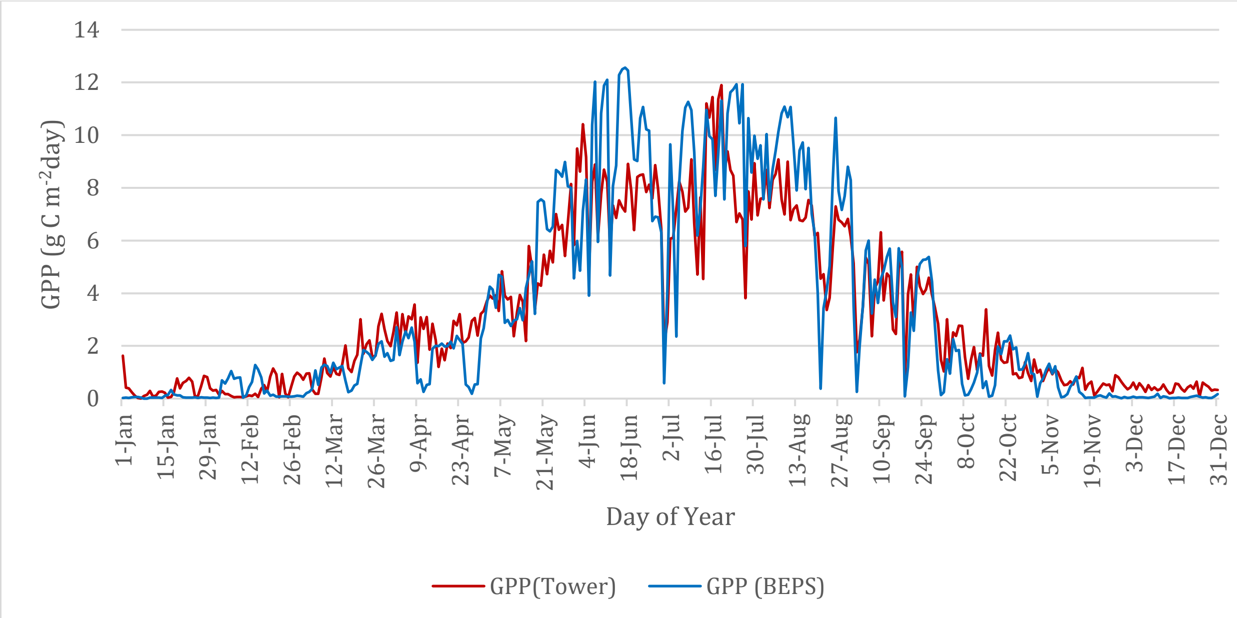

Figure 14. BEPS model and eddy covariance tower measurements in 2017.

The daily BEPS GPP values are plotted against the tower based GPP values (Figure 15) with a strong, close to 1:1 line relationship with a very good R square value of 0.86.

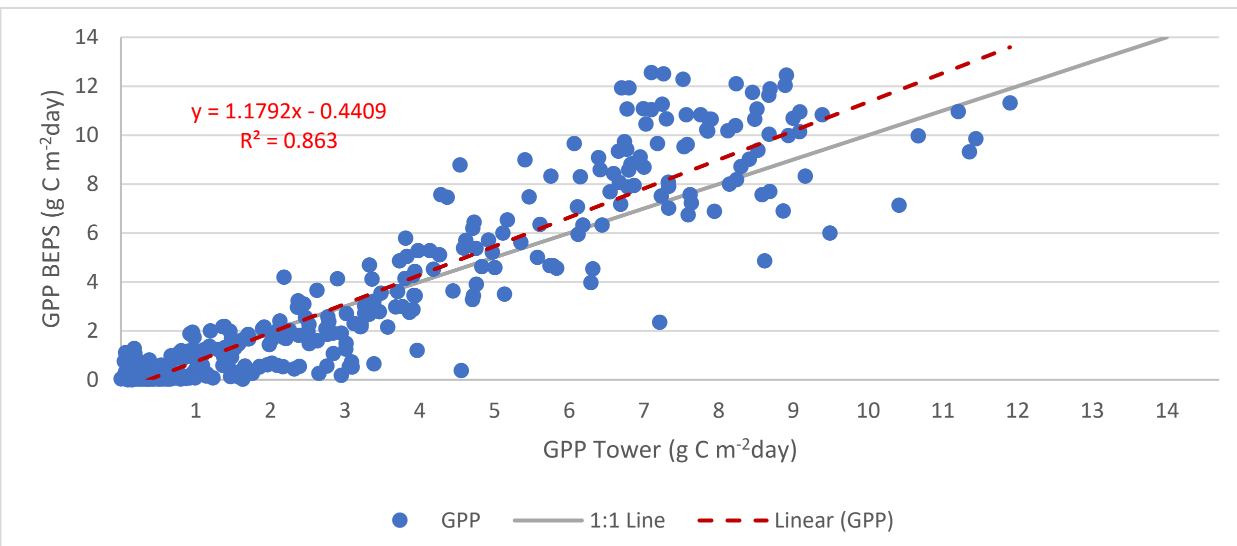

Figure 15. Comparison between BEPS and tower daily GPP estimates in 2017 (The solid line is 1:1 line and dashed one is linear fit regression line).

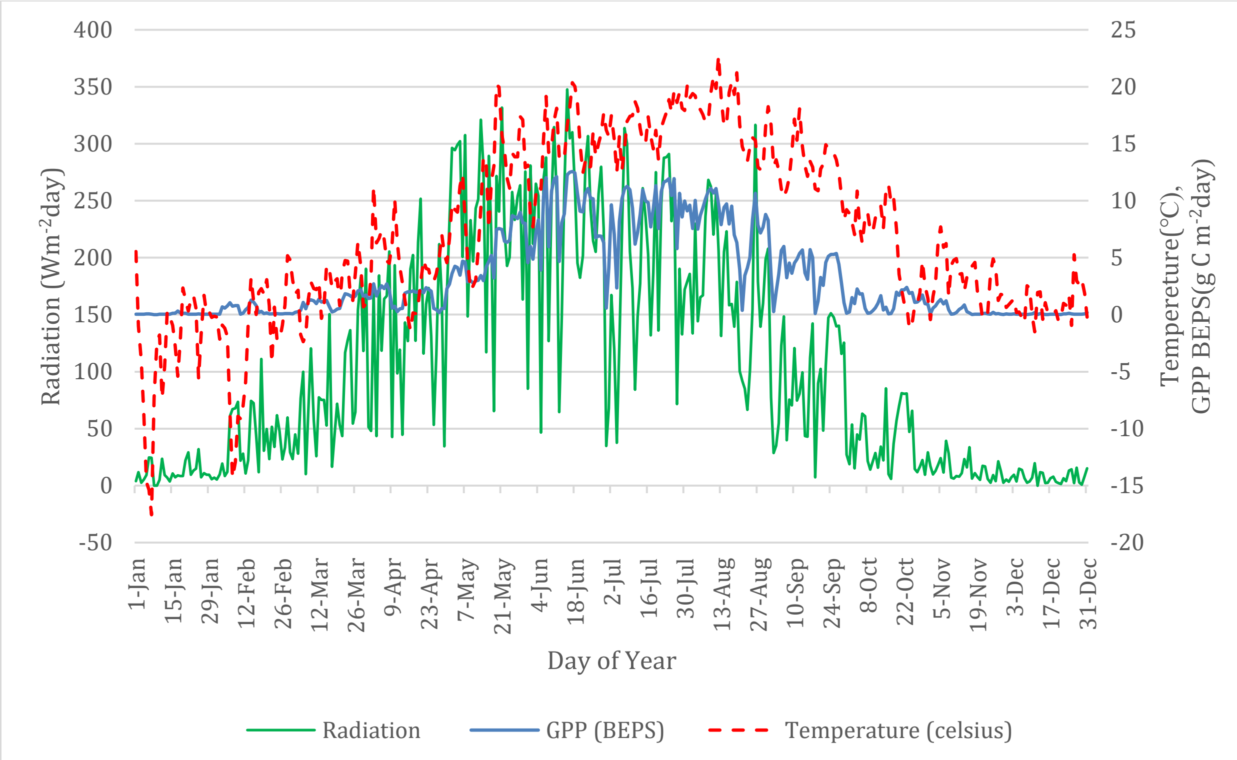

Figure 16. Radiation and temperature impact on BEPS GPP in 2017.

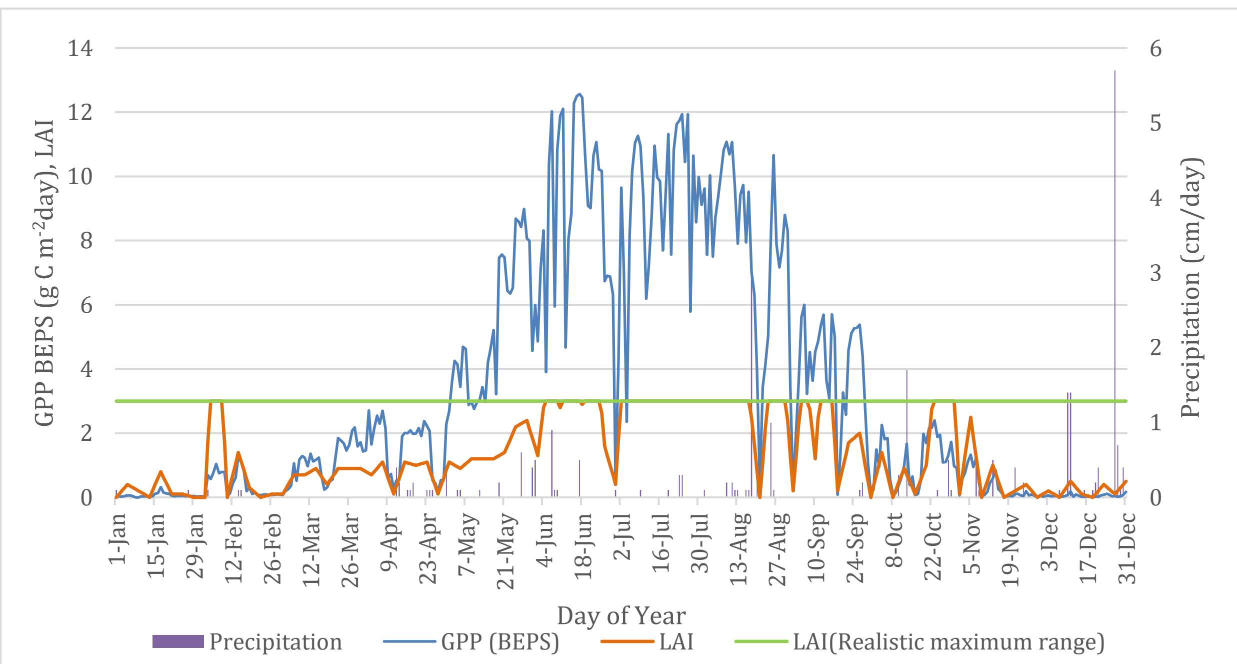

Figure 17. Seasonality impact on BEPS GPP in 2017.

The expected GPP rate was higher for 2016 as it had cold, and wet weather condition based on Table 2. The results were less convincing compared to other years with the 23.12% underestimation of the annual sum of GPP estimates by BEPS compared to tower-based estimates. While there was a close relationship with a very little difference between BEPS and tower estimates in the second half of the growing season (Figure 18), there was an unrealistic drop in BEPS GPP retrievals from the middle of the June till the third week of July. This drop in GPP values was caused by the missing humidity values during that period (Figure A2 in the Annex). Additionally, more clear evidence can be seen if the daily BEPS GPP values are plotted against the tower GPP values with the dropped humidity input data and without the dropped humidity input data. With all days of year included in Figure 19, it shows a diverging relationship from the 1:1 line and the R square value is 0.7, while the omission of days with missing humidity inputs improves the R square value to 0.81.

On the other hand, the GPP BEPS was over-estimated with very high values from the last week of May to second week of June. It was caused by the apparently over-estimated MODIS LAI values at the very beginning of the growing season when the LAI compared to the probable actual LAI values at the site. At the beginning of the year till half of February the LAI values were 0 (Figure 21) which resulted in zero value GPP estimates from BEPS at the beginning of the year to mid-February (Figure 18). But, except from the LAI impact and the humidity input issue, second half of the year showed BEPS GPP values to provide a close match with the expected, tower-based observations. GPP also matches well with low temperature (Figure 20) and high precipitation (Figure 21) during this period.

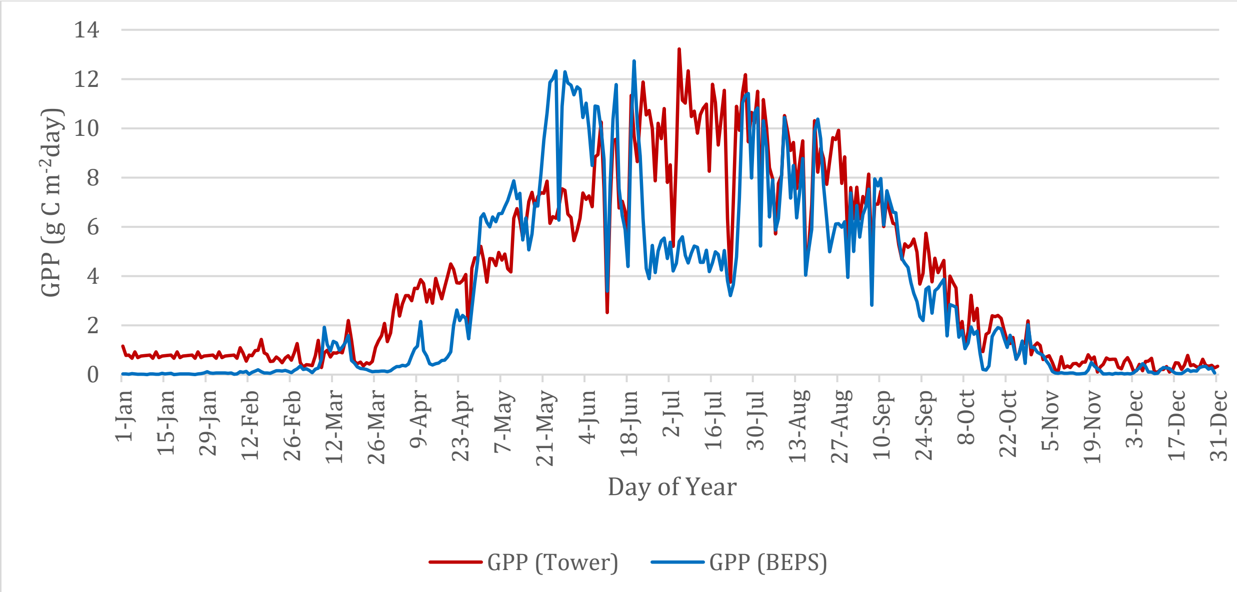

Figure 18. BEPS model and eddy covariance tower measurements in 2016.

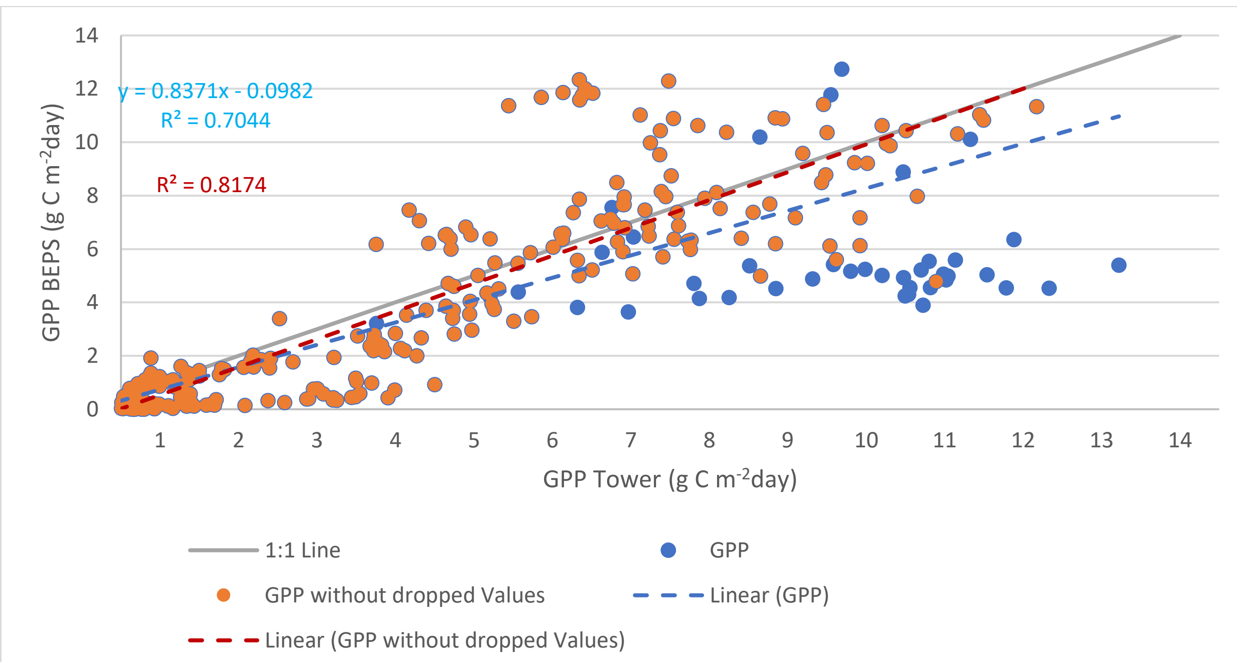

Figure 19. Comparison between BEPS and tower daily GPP estimates in2016 (The solid line is 1:1 line and dashed lines are linear fit regression lines with and without dropped values).

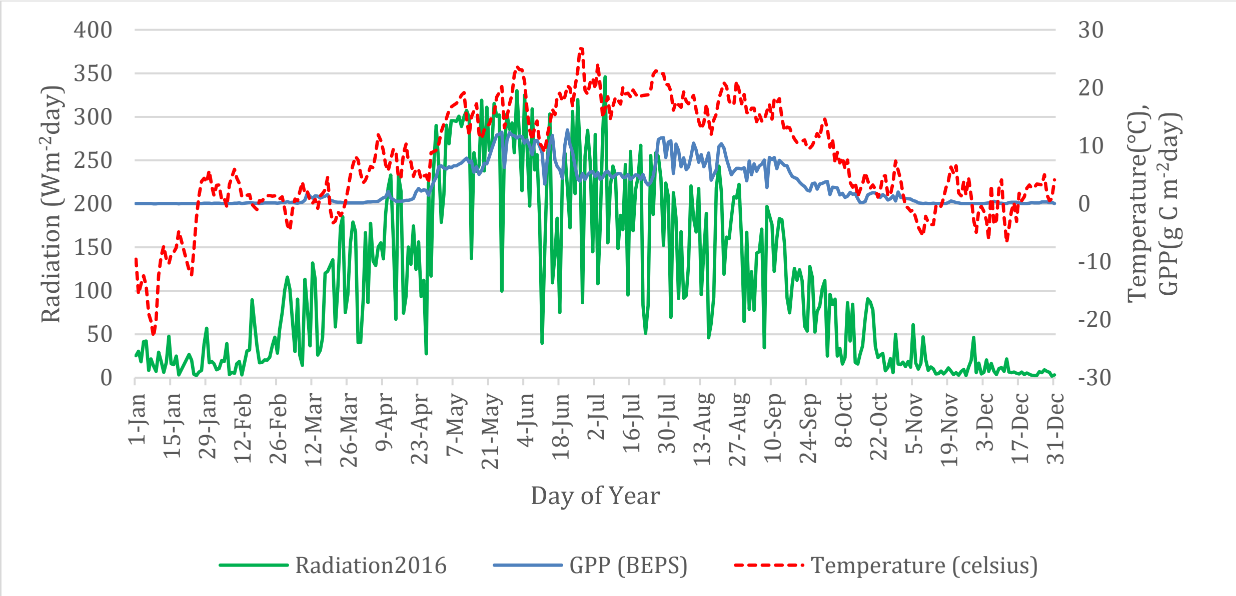

Figure 20. Radiation and temperature impact on GPP in 2016.

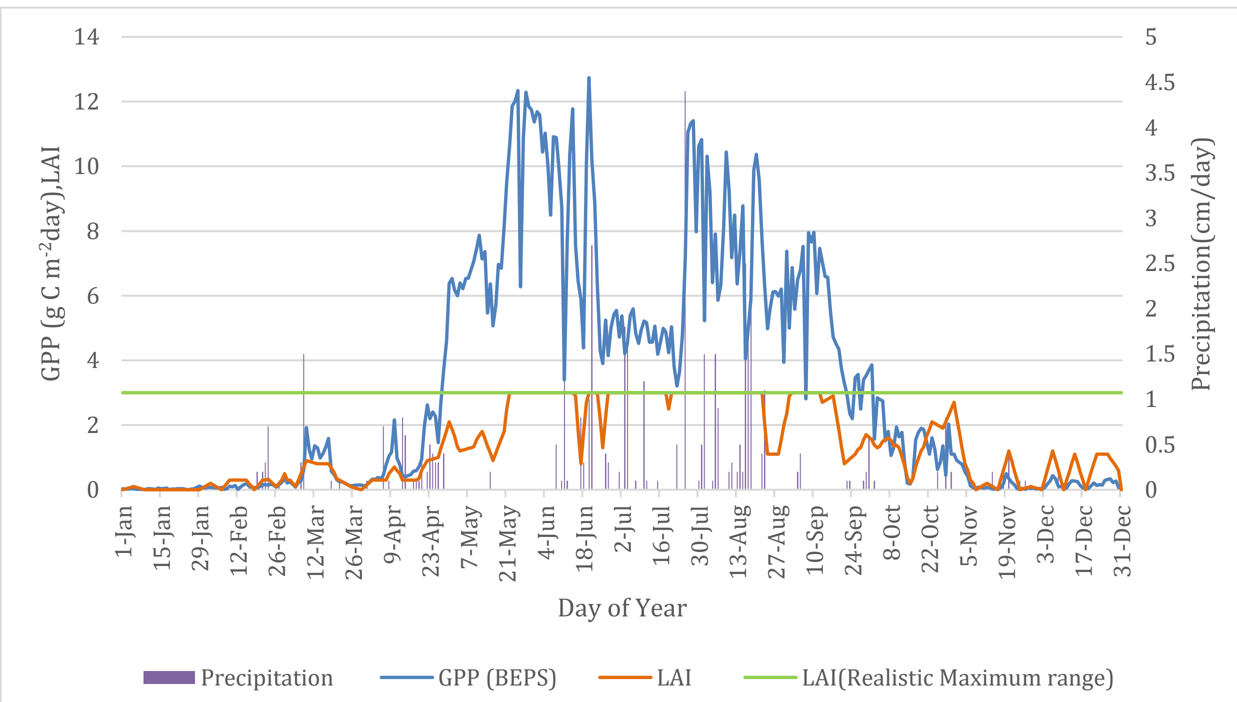

Figure 21. Seasonality impact on GPP in 2016.

4. Conclusion

GPP estimation is very important topic for global climate change as evidenced by numerous studies carried over different regions. Different strategies and models can be applied to achieve a good performance. The BEPS model has been previously applied in Canada (Liu et al., 2002), various region of China (Li et al., 2016), select sites around Europe (Zhang et al., 2018), USA (Zhang et al., 2012). In this study, the BEPS model was tested for estimating GPP in a hemi-boreal region in Estonia to evaluate its performance and reliability for future use.

Zhu et al. (2018) noted that the GPP estimation by BEPS model causes 34% of underestimation for grassland ecosystem biomes in temperate, tropical, and alpine sites. To reduce the underestimation problem, Zhu et al. (2018) recommended using the long-term remote sensing and meteorological data which should be used with consideration of different seasonal courses and especially a drought. However, in the present study BEPS model performed well and provided less significant underestimation or overestimation for hemi-boreal forest.

The objective of this study has been achieved and research questions were answered with proper analysis and evidence. Based on the analysis of BEPS, GPP results for different years on Estonian hemi-boreal conditions, it can be concluded BEPS is a robust and efficient tool for GPP estimation in the region. From the perspective of BEPS model's tracking of the GPP changes with season and inter-annual variation, it is found BEPS model can track the changes very well even during extreme weather condition like drought, given the model is provided with reasonable input values.

It shall be noted that BEPS is particularly sensitive to the quality and reliability of input LAI values. Feng et al. (2007) also found that LAI accuracy had a significant impact on NPP estimation as well as GPP estimation in China. From the analysis in this study, it is shown that the reliability of MODIS LAI product had a substantial effect on the quality of GPP estimates by the BEPS model in the hemi-boreal region as well. Regarding other factors, the analysis also showed that the BEPS is correctly responding particularly to the changes in humidity and incoming radiation. The use of unbiased, non-interpolated meteorological data along the correct LAI, clumping index input shall lead to good quality GPP estimates by the BEPS model over Estonia, the possible next step.

Summary

Estimating hemi-boreal forest productivity with a process-based BEPS model and multi-source Earth Observation data

Author- Fariha Harun

Gross primary productivity (GPP) plays a major role in the field of global carbon cycle as well as climate change (Feng et al., 2007). Accurate and continuous GPP estimation is very important to provide an idea about the terrestrial ecosystem's sustainability in the long term (Shi et al., 2017).

The aim of this study is to evaluate potential suitability of Boreal Ecosystem Productivity Simulator (BEPS) model for GPP estimation over hemi-boreal forests using the available GPP measurements.

This study sought to answer three research questions:

a. How spatially heterogenous is the Soontaga flux tower area?
b. How much reliable GPP information can be simulated by the BEPS compared to estimates obtained with the tower eddy covariance measurements taken at the Soontaga site?
c. How well can the BEPS model track the GPP changes with season and inter-annual variation?

BEPS was originally tailored for Canadian boreal forest conditions with an input from remote sensing data (Chen et al., 1999; Feng et al., 2007). MODIS leaf area index (LAI), land cover, clumping index and daily meteorological information were used as model inputs in this study.

This study was performed at Soontaga Flux tower area (58°01'24 "N, 26°04'15"E), which is a dry hemi-boreal forest in Estonia, over the period of 2016 to 2019. First, the spatial representativeness of the flux tower area was evaluated using the surface albedo retrievals from a 30 m spatial resolution Landsat data as an input to the gamma variance model. The Soontaga area was found to be spatially representative within 500 m radius from the flux tower, the nominal resolution of the MODIS remote sensing data products used in this study.

Next, based on the analysis of BEPS GPP result for different years on Estonian hemi-boreal conditions, it can be concluded BEPS is a robust and efficient tool for GPP estimation in the region.

From the perspective of BEPS model's tracking of the GPP changes with season and inter-annual variation, it is found from the analysis that, BEPS model can track the changes very well even during extreme weather conditions such as drought, given the model is provided with reasonable input values. BEPS model was found to be particularly sensitive to the quality and reliability of input LAI values. Regarding other factors, the analysis also showed that the BEPS is correctly responding particularly to the changes in humidity and incoming radiation. The use of unbiased, non-interpolated meteorological data along the correct LAI, clumping index input shall lead to good quality GPP estimates by the BEPS model over Estonia, the possible next step.

Kokkuvõte

Hemi-boreaalse metsa tootlikkuse hindamine protsessipõhise BEPS-mudeli ja mitme allikaga Maa vaatlusandmete abil

Autor-Fariha Harun

Primaarproduktsioon mängib ülemaailmses süsinikuringes ja kliimamuutustes suurt rolli (Feng et al., 2007). Täpne ja järjekestev primaarproduktsiooni hindamine on väga oluline, andmaks ettekujutust maismaaökosüsteemide jätkusuutlikkusest pikas perspektiivis (Shi et al., 2017).

Antud uurimuse eesmärk on hinnata boreaalse ökosüsteemi tootlikkuse simulaatori (BEPS) mudeli potentsiaalset sobivust primaarproduktsiooni hindamiseks hemiboreaalsetes metsades, kasutades olemasolevaid mõõtmistulemusi.

Antud töös püstitati kolm uurimisküsimust:

a) Milline on Soontaga uurimismasti ala ruumiline heterogeensus?
b) Kui täpselt ja usaldusväärselt saab hinnata primaarproduktsiooni BEPS-mudeliga, võrreldes turbulentse kovariatsiooni meetodil saadud mõõtmistulemustega Soontaga uurimisjaamast?
c) Kui hästi jälgib BEPS-mudel primaarproduktsiooni sesoonseid muutusi ja aastatevahelisi variatsioone?

BEPS-mudel kohandati algselt Kanada boreaalsete metsatingimuste jaoks, kasutades kaugseire sisendandmeid (Chen et al., 1999; Feng et al., 2007). Antud uurimuses kasutati mudeli sisendandmetena lehepinnaindeksit, maakasutust, *clumping* indeksit ja igapäevaseid ilmaandmeid.

Käesolev uurimus viidi läbi ajavahemikul 2016–2019 Soontaga gaasivoogude mõõtmiseks kasutatava uurimismasti alal (58°01'24''N, 26°04'15''E), mis esindab kuiva hemiboreaalset metsa Eestis. Esmalt hinnati uurimismasti ala ruumilist sobivust, kasutades gamma dispersioonimudeli sisendina pinnaalbeedo väljavõtteid 30-meetrise ruumilise lahutusvõimega Landsat andmestikust. Leiti, et Soontaga piirkond on ruumiliselt representatiivne 500 m raadiuses uurimismastist, mis on selles uuringus kasutatud MODIS-kaugseire andmetoodete nominaalne lahutusvõime.

Teiseks uuriti BEPS-mudelit kasutades primaarproduktsiooni muutusi mitme aasta lõikes Eesti hemiboreaalsetes tingimustes. Tulemustest saab järeldada, et Soontaga piirkonnas on BEPS tõhus ja võimekas vahend primaarproduktsiooni hindamiseks. Uurides BEPS-mudeli võimekust jälgida primaarproduktsiooni sesoonseid muutusi ja aastatevahelisi variatsioone, leiti, et sobilike sisendväärtuste olemasolul suudab mudel muutusi väga edukalt jälgida isegi ekstreemsete ilmastikutingimuste, näiteks põua korral. Leiti ka, et BEPS-mudel on eriti tundlik lehepinnaindeksi sisendväärtuste kvaliteedi ja usaldusväärtuse suhtes. Analüüs näitas, et BEPS-mudel reageerib korrektselt ka muude tegurite muutuste osas, eriti õhuniiskuse ja sissetuleva kiirguse puhul. Järgmiseks sammuks antud teema uurimises võiks olla erapooletute ja interpoleerimata meteoroloogiliste andmete ning korrektsete lehepinna- ja *clumping* indeksi kasutamine sisendandmetena BEPS-mudelisse. See võimaldaks anda korrektse ja usaldusväärse hinnangu Eesti primaarproduktsioonile.

Acknowledgements

Heartfelt thanks to my supervisors Dr. Jan Pisek and Dr. Kaido Soosaar for their guidance, support, and reviewed feedback for this research. I would like to thank Alisa Krasnova for supporting me with the tower measured data for validating my model performance and Mohammad Kamil Ali Sardar for providing me with the meteorological input data. Sincere thanks to my family for supporting me throughout the study.

References

Anav, A., Friedlingstein, P., Kidston, M., Bopp, L., Ciais, P., Cox, P., Jones, C., Jung, M., Myneni, R., & Zhu, Z. (2013). Evaluating the land and ocean components of the global carbon cycle in the CMIP5 earth system models. *Journal of Climate*, *26*(18), 6801–6843. https://doi.org/10.1175/JCLI-D-12-00417.1

Beer, C., Reichstein, M., Tomelleri, E., Ciais, P., Jung, M., Carvalhais, N., Rödenbeck, C., Arain, M. A., Baldocchi, D., Bonan, G. B., Bondeau, A., Cescatti, A., Lasslop, G., Lindroth, A., Lomas, M., Luyssaert, S., Margolis, H., Oleson, K. W., Roupsard, O., … Papale, D. (2010). Terrestrial gross carbon dioxide uptake: Global distribution and covariation with climate. *Science*, *329*(5993), 834–838. https://doi.org/10.1126/science.1184984

Bonan, G. B. (1995). Land-atmosphere CO_2 exchange simulated by a land surface process model coupled to an atmospheric general circulation model. *Journal of Geophysical Research*, *100*(D2), 2817. https://doi.org/10.1029/94JD02961

Chen, J. M., Liu, J., Cihlar, J., & Goulden, M. L. (1999). Daily canopy photosynthesis model through temporal and spatial scaling for remote sensing applications. *Ecological Modelling*, *124*(2–3), 99–119. https://doi.org/10.1016/s0304-3800(99)00156-8

Chen, Jing M., Mo, G., Pisek, J., Liu, J., Deng, F., Ishizawa, M., & Chan, D. (2012). Effects of foliage clumping on the estimation of global terrestrial gross primary productivity. *Global Biogeochemical Cycles*, *26*(1). https://doi.org/10.1029/2010GB003996

Feng, X., Liu, G., Chen, J. M., Chen, M., Liu, J., Ju, W. M., Sun, R., & Zhou, W. (2007). Net primary productivity of China's terrestrial ecosystems from a process model driven by remote sensing. *Journal of Environmental Management*, *85*(3), 563–573. https://doi.org/10.1016/j.jenvman.2006.09.021

He, L., Chen, J. M., Pisek, J., Schaaf, C. B., & Strahler, A. H. (2012). Global clumping index map derived from the MODIS BRDF product. *Remote Sensing of Environment*, *119*, 118–130. https://doi.org/10.1016/j.rse.2011.12.008

Heiskanen, J., Rautiainen, M., Stenberg, P., Mõttus, M., Vesanto, V. H., Korhonen, L., & Majasalmi, T. (2012). Seasonal variation in MODIS LAI for a boreal forest area in Finland. *Remote Sensing of Environment*, *126*, 104–115. https://doi.org/10.1016/j.rse.2012.08.001

Krasnova, A., Kukumägi, M., Mander, Ü., Torga, R., Krasnov, D., Noe, M., Ostonen, I., Püttsepp, Ü., Killian, H., Uri, V., Lõhmus, K., & Sõber, J. (2019). *Agricultural and Forest Meteorology Carbon exchange in a hemiboreal mixed forest in relation to tree species composition*. *275*(November 2018), 11–23. https://doi.org/10.1016/j.agrformet.2019.05.007

Li, X., Zhu, Z., Zeng, H., & Piao, S. (2016). Estimation of gross primary production in China (1982-2010) with multiple ecosystem models. *Ecological Modelling*, *324*, 33–44. https://doi.org/10.1016/j.ecolmodel.2015.12.019

Liang, S., Shuey, C. J., Russ, A. L., Fang, H., Chen, M., Walthall, C. L., Daughtry, C. S. T., & Hunt, R. (2003). Narrowband to broadband conversions of land surface albedo: II. Validation. *Remote Sensing of Environment*, *84*(1), 25–41. https://doi.org/10.1016/S0034-4257(02)00068-8

Liu, J., Chen, J. M., Cihlar, J., & Chen, W. (1999). Net primary productivity distribution in the BOREAS region from a process model using satellite and surface data. *Journal of Geophysical Research Atmospheres*, *104*(D22), 27735–27754. https://doi.org/10.1029/1999JD900768

Liu, J., Chen, J. M., Cihlar, J., & Chen, W. (2002). Net primary productivity mapped for Canada at 1-km resolution. *Global Ecology and Biogeography*, *11*(2), 115–129. https://doi.org/10.1046/j.1466-822X.2002.00278.x

Liu, J., Chen, J. M., Cihlar, J., & Park, W. M. (1997). A process-based boreal ecosystem productivity simulator using remote sensing inputs. *Remote Sensing of Environment*, *62*(2), 158–175. https://doi.org/10.1016/S0034-4257(97)00089-8

Liu, S., Zhuang, Q., He, Y., Noormets, A., Chen, J., & Gu, L. (2016). Evaluating atmospheric CO2 effects on gross primary productivity and net ecosystem exchanges of terrestrial ecosystems in the conterminous United States using the AmeriFlux data and an artificial neural network approach. *Agricultural and Forest Meteorology*, *220*, 38–49. https://doi.org/10.1016/j.agrformet.2016.01.007

Lloyd, J., & Taylor, J. A. (1994). On the Temperature Dependence of Soil Respiration. In *Ecology* (Vol. 8, Issue 3). https://www.jstor.org/stable/2389824

Ma, L., Bicking, S., & Müller, F. (2019). Mapping and comparing ecosystem service indicators of global climate regulation in Schleswig-Holstein, Northern Germany. *Science of the Total Environment*, *648*, 1582–1597. https://doi.org/10.1016/j.scitotenv.2018.08.274

Nilson, T. (1971). A theoretical analysis of the frequency of gaps in plant stands. *Agricultural Meteorology*, *8*(C), 25–38. https://doi.org/10.1016/0002-1571(71)90092-6

Prentice, I. C., Heimann, M., & Sitch, S. (2000). The carbon balance of the terrestrial biosphere: Ecosystem models and atmospheric observations. *Ecological Applications*, *10*(6), 1553–1573. https://doi.org/10.1890/1051-0761(2000)010[1553:TCBOTT]2.0.CO;2

Reichstein, M., Falge, E., Baldocchi, D., Papale, D., Aubinet, M., Berbigier, P., Bernhofer, C., Buchmann, N., Gilmanov, T., Granier, A., Grünwald, T., Havránková, K., Ilvesniemi, H., Janous, D., Knohl, A., Laurila, T., Lohila, A., Loustau, D., Matteucci, G., … Valentini, R. (2005). On the separation of net ecosystem exchange into assimilation and ecosystem respiration: Review and improved algorithm. *Global Change Biology*, *11*(9), 1424–1439. https://doi.org/10.1111/j.1365-2486.2005.001002.x

Román, M. O., Schaaf, C. B., Woodcock, C. E., Strahler, A. H., Yang, X., Braswell, R. H., Curtis, P. S., Davis, K. J., Dragoni, D., Goulden, M. L., Gu, L., Hollinger, D. Y., Kolb, T. E., Meyers, T. P., Munger, J. W., Privette, J. L., Richardson, A. D., Wilson, T. B., & Wofsy, S. C. (2009). The MODIS (Collection V005) BRDF/albedo product: Assessment of spatial representativeness over forested landscapes. *Remote Sensing of Environment*, *113*(11), 2476–2498. https://doi.org/10.1016/j.rse.2009.07.009

Shi, H., Li, L., Eamus, D., Huete, A., Cleverly, J., Tian, X., Yu, Q., Wang, S., Montagnani, L., Magliulo, V., Rotenberg, E., Pavelka, M., & Carrara, A. (2017). Assessing the ability of MODIS EVI to estimate terrestrial ecosystem gross primary production of multiple land cover types. *Ecological Indicators*, *72*, 153–164. https://doi.org/10.1016/j.ecolind.2016.08.022

The heat budget of the earth ' s surface deduced from space (R . B . Smith ; Version : March , 2010) 2 . Solar Radiation (VIS and SWIR) a . Basic equations. (2010). *Terrain*, *0*, 1–10.

Wang, Z., Schaaf, C. B., Chopping, M. J., Strahler, A. H., Wang, J., Román, M. O., Rocha, A. V., Woodcock, C. E., & Shuai, Y. (2012). Evaluation of Moderate-resolution Imaging Spectroradiometer (MODIS) snow albedo product (MCD43A) over tundra. *Remote Sensing of Environment*, *117*, 264–280. https://doi.org/10.1016/j.rse.2011.10.002

Wang, Z., Schaaf, C. B., Strahler, A. H., Chopping, M. J., Román, M. O., Shuai, Y., Woodcock, C. E., Hollinger, D. Y., & Fitzjarrald, D. R. (2014). Evaluation of MODIS albedo product (MCD43A) over grassland, agriculture and forest surface types during dormant and snow-covered periods. *Remote Sensing of Environment*, *140*, 60–77. https://doi.org/10.1016/j.rse.2013.08.025

Wang, Z., Schaaf, C. B., Sun, Q., Kim, J., Erb, A. M., Gao, F., Román, M. O., Yang, Y., Petroy, S., Taylor, J. R., Masek, J. G., Morisette, J. T., Zhang, X., & Papuga, S. A. (2017). International Journal of Applied Earth Observation and Geoinformation Monitoring land surface albedo and vegetation dynamics using high spatial and temporal resolution synthetic time series from Landsat and the MODIS BRDF / NBAR / albedo product. *International Journal of Applied Earth Observations and Geoinformation*, *59*, 104–117. https://doi.org/10.1016/j.jag.2017.03.008

Wu, C., Munger, J. W., Niu, Z., & Kuang, D. (2010). Remote Sensing of Environment Comparison of multiple models for estimating gross primary production using MODIS and eddy covariance data in Harvard Forest. *Remote Sensing of Environment*, *114*(12), 2925–2939. https://doi.org/10.1016/j.rse.2010.07.012

Wutzler, T., Lucas-Moffat, A., Migliavacca, M., Knauer, J., Sickel, K., Šigut, L., Menzer, O., & Reichstein, M. (2018). Basic and extensible post-processing of eddy covariance flux data with REddyProc. *Biogeosciences*, *15*(16), 5015–5030. https://doi.org/10.5194/bg-15-5015-2018

Xiao, J., Chevallier, F., Gomez, C., Guanter, L., Hicke, J. A., Huete, A. R., Ichii, K., Ni, W., Pang, Y., Rahman, A. F., Sun, G., Yuan, W., Zhang, L., & Zhang, X. (2019). Remote sensing of the terrestrial carbon cycle: A review of advances over 50 years. *Remote Sensing of Environment*, *233*(September), 111383. https://doi.org/10.1016/j.rse.2019.111383

Xiao, X., Zhang, Q., Hollinger, D., Aber, J., & Iii, B. M. (2005). MODELING GROSS PRIMARY PRODUCTION OF AN EVERGREEN NEEDLELEAF FOREST USING MODIS AND CLIMATE DATA. In *Ecological Applications* (Vol. 15, Issue 3). http://public.ornl.gov/ameriflux/Data/index.cfm

Zhang, F., Chen, J. M., Chen, J., Gough, C. M., Martin, T. A., & Dragoni, D. (2012). Evaluating spatial and temporal patterns of MODIS GPP over the conterminous U.S. against flux measurements and a process model. *Remote Sensing of Environment*, *124*, 717–729. https://doi.org/10.1016/j.rse.2012.06.023

Zhang, S., Zhang, J., Bai, Y., Koju, U. A., Igbawua, T., Chang, Q., Zhang, D., & Yao, F. (2018). Evaluation and improvement of the daily boreal ecosystem productivity simulator in simulating gross primary productivity at 41 flux sites across Europe. *Ecological Modelling*, *368*, 205–232. https://doi.org/10.1016/j.ecolmodel.2017.11.023

Zhu, X., Pei, Y., Zheng, Z., Dong, J., & Zhang, Y. (2018). *Underestimates of Grassland Gross Primary Production in MODIS Standard Products*. *November*. https://doi.org/10.3390/rs10111771

Web Reference

Estonian Environment Agency (KAUR), https://www.keskkonnaagentuur.ee/en, (last viewed 26.12.2020)

Estonian Weather Service, https://www.ilmateenistus.ee/?lang = en, (last viewed 17.04.2021)

Annex:

Annex 1: Yearly wind speed from 2016 to 2019 in daily average values

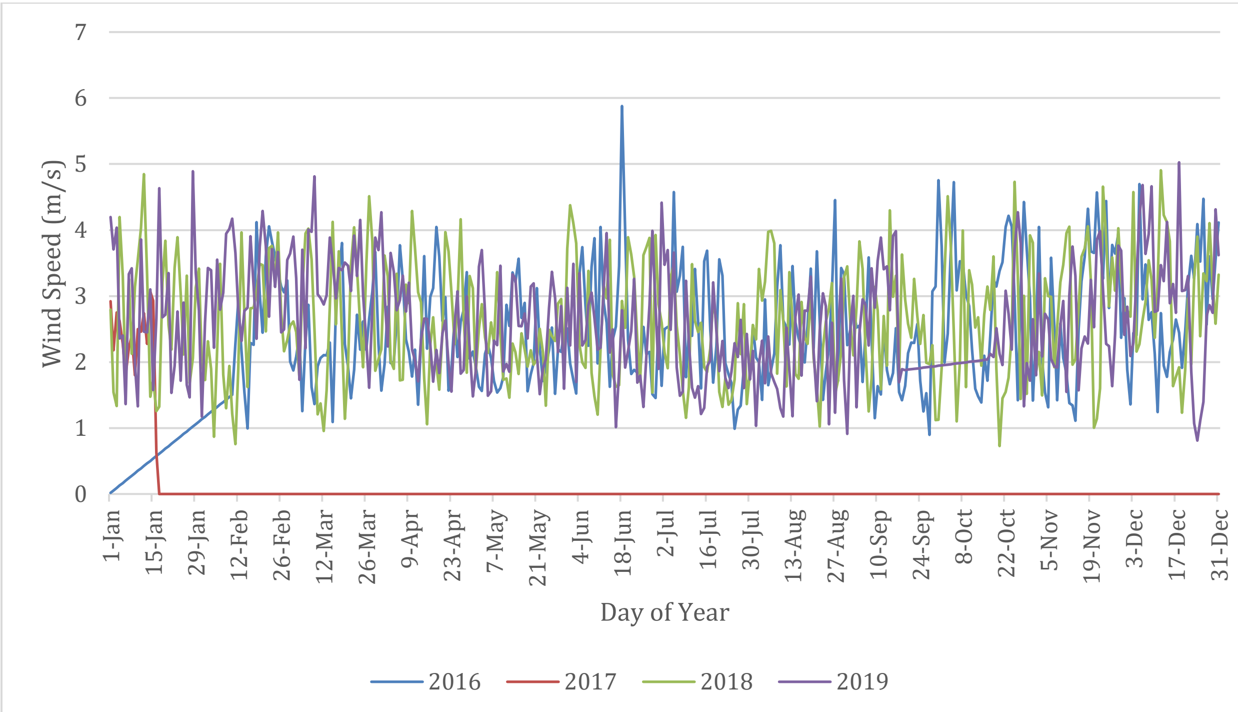

Figure A1. Daily average wind speed at Soontaga flux site during the period 2016-2019.

Annex 2: Daily humidity values with comparison of yearly data from 2016 to 2019

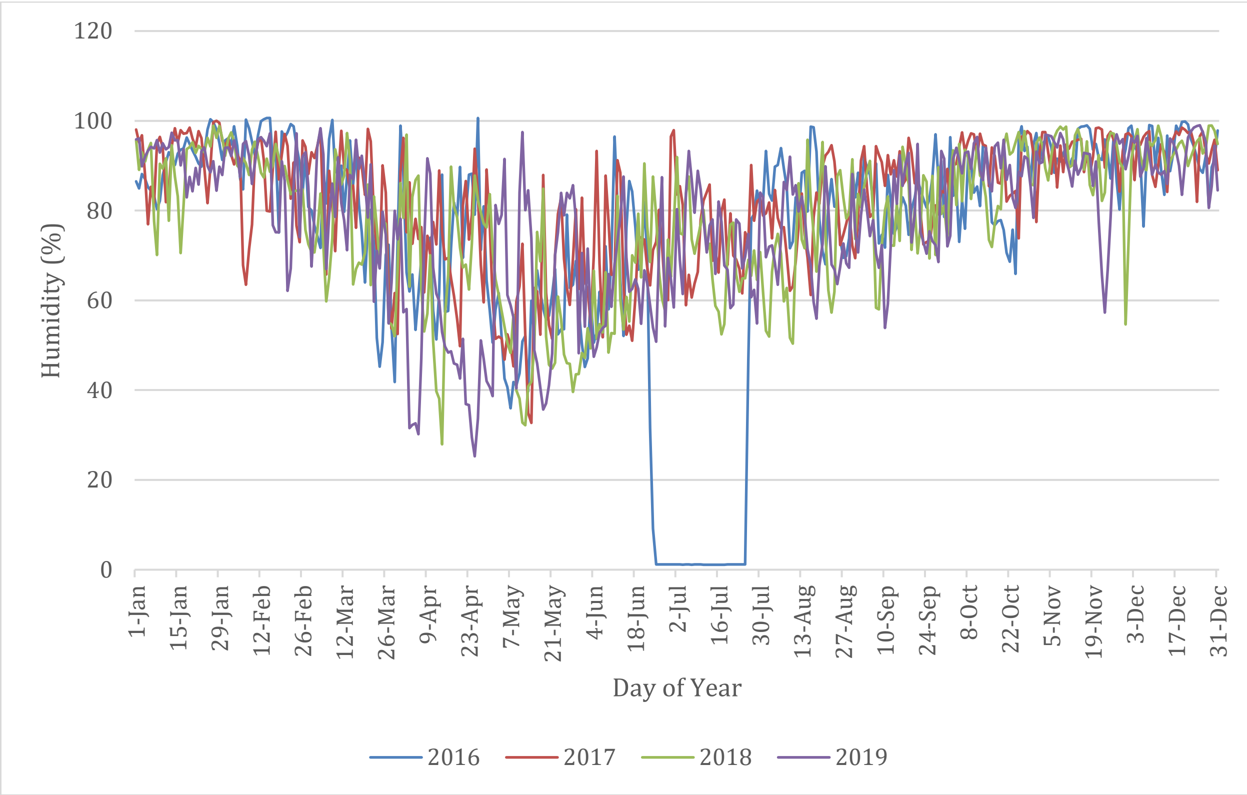

Figure A2. Daily humidity at Soontaga flux site during the period 2016-2019.

Annex 3: Daily radiation values

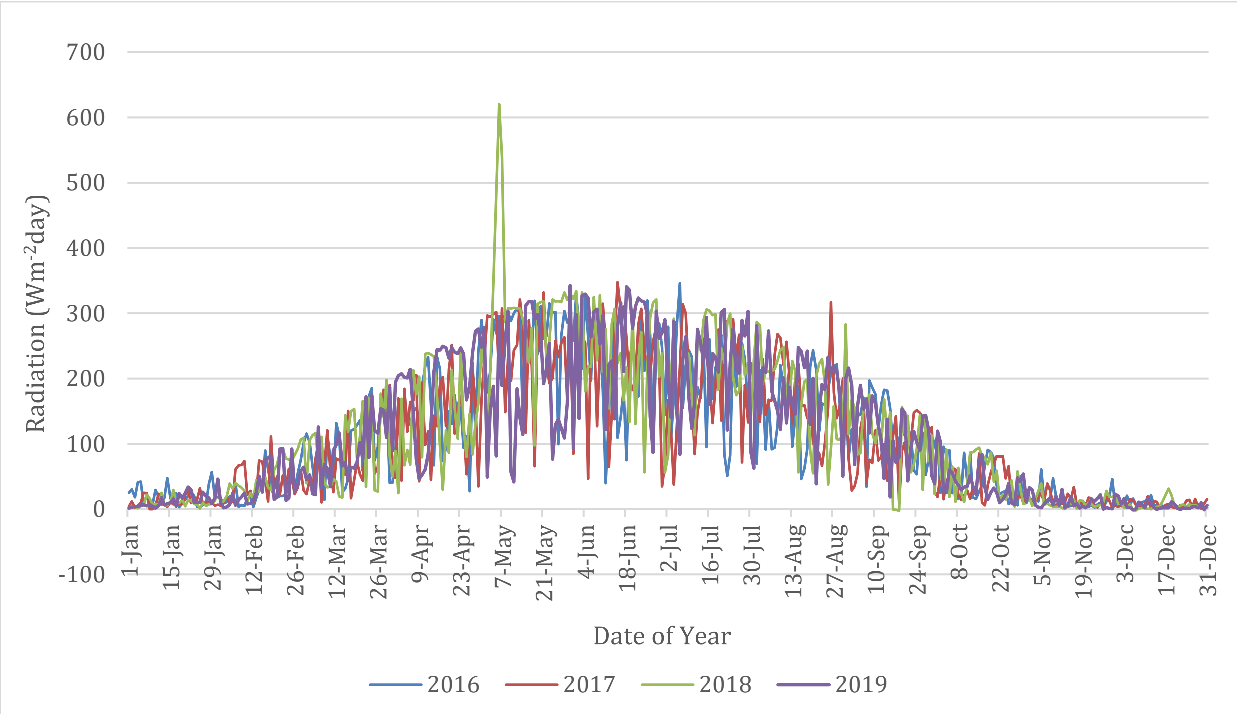

Figure A3. Daily average of radiation values at Soontaga flux site during the period 2016-2019.

Annex 4: Low irradiation impact on BEPS GPP and Tower GPP for 2018.

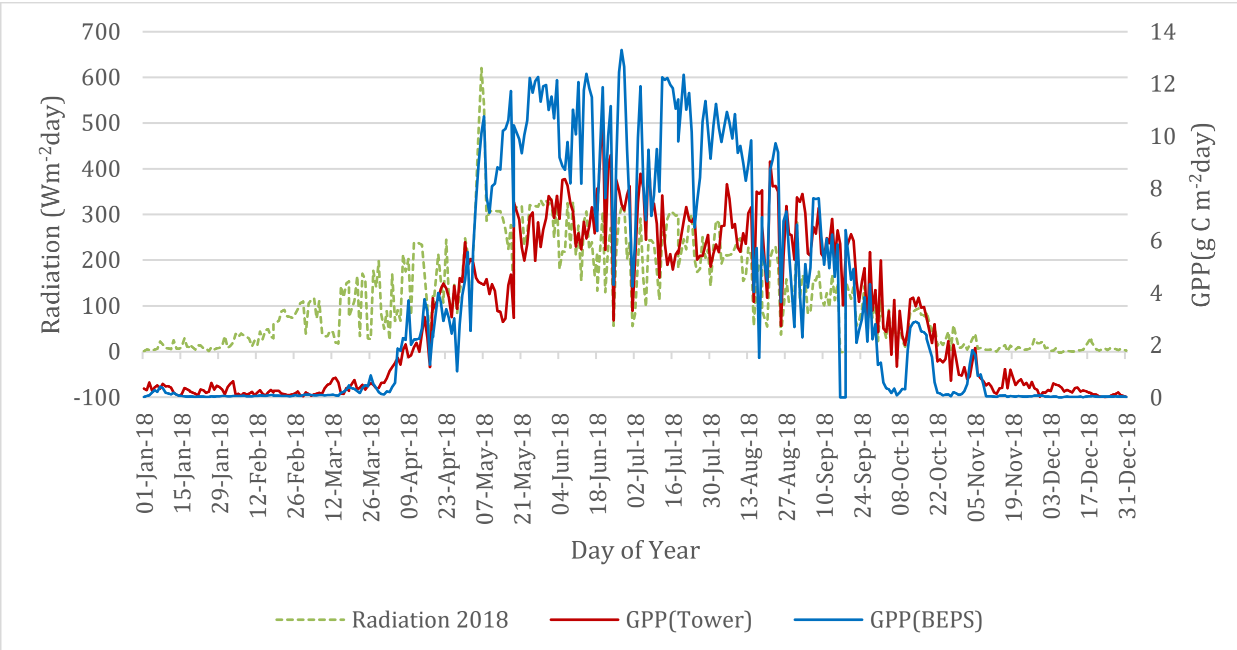

Figure A4. Effect of lower irradiation periods on the daily GPP fluctuation in 2018.

Annex 5: Low irradiation impact on BEPS GPP and Tower GPP for 2017

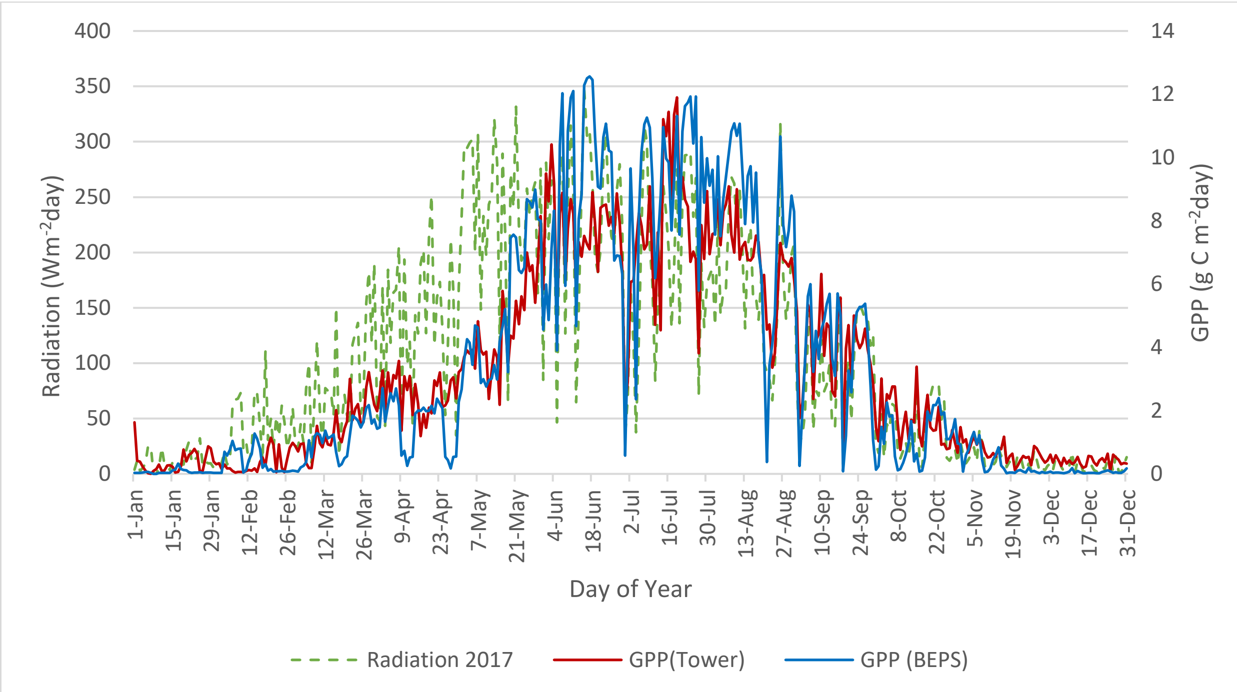

Figure A5. Effect of lower irradiation periods on the daily GPP fluctuation in 2017.

Annex 6: Low irradiation impact on BEPS GPP and Tower GPP for 2016.

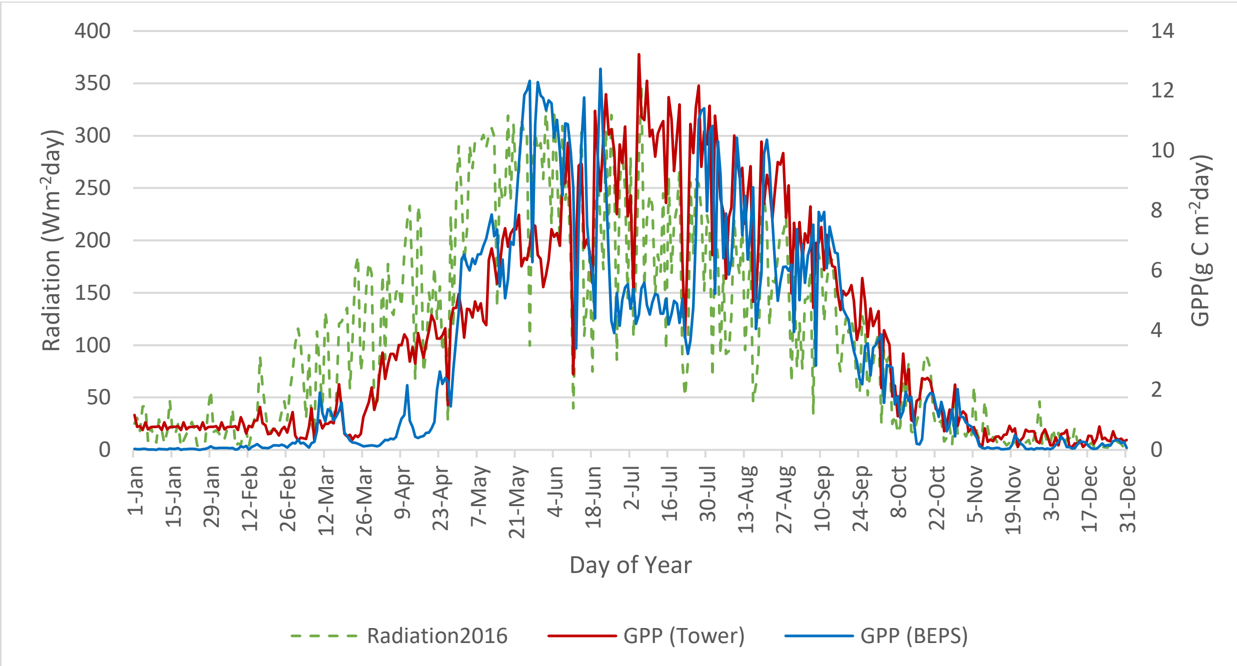

Figure A6. Effect of lower irradiation periods on the daily GPP fluctuation in 2016.

Annex 7: GPP production during growing season (Comparing BEPS GPP and Tower GPP)

Year (Mid-April-Mid-September)	GPP BEPS (g Cm^{-2})	GPP Tower (g Cm^{-2})	Difference (%)
2019	1176.51	1055.50	1.21
2018	1256.78	920.01	3.37
2017	1043.11	920.05	1.23
2016	900.30	916.11	-0.16

Non-exclusive license to reproduce thesis and make thesis public

I, **Fariha Harun** (date of birth 27.05.1996),

herewith grant the University of Tartu a free permit (non-exclusive licence) to reproduce, for the purpose of preservation, including for adding to the DSpace digital archives until the expiry of the term of copyright,

Estimating hemi-boreal forest productivity with a process-based BEPS model and multi-source Earth Observation data supervised by **Dr. Jan Pisek** and **Dr. Kaido Soosaar**

2. I grant the University of Tartu a permit to make the work specified in p. 1 available to the public via the web environment of the University of Tartu, including via the DSpace digital archives, under the Creative Commons licence CC BY NC ND 3.0, which allows, by giving appropriate credit to the author, to reproduce, distribute the work and communicate it to the public, and prohibits the creation of derivative works and any commercial use of the work until the expiry of the term of copyright.

3. I am aware of the fact that, the author retains the rights specified in p. 1 and 2.

4. I certify that granting the non-exclusive licence does not infringe other persons' intellectual property rights or rights arising from the personal data protection legislation

Fariha Harun

24.05.2021